Oxadiazole-Based Cell Permeable Macrocyclic Transition State Inhibitors of Norovirus 3CL Protease

Vishnu C. Damalanka,[†] Yunjeong Kim,[‡] Kevin R. Alliston,[†] Pathum M. Weerawarna,[†] Anushka C. Galasiti Kankanamalage,[†] Gerald H. Lushington,[||] Nurjahan Mehzabeen,[§] Kevin P. Battaile,[⊥] Scott Lovell,[§] Kyeong-Ok Chang,*[‡] and William C. Groutas*[†]

[†]Department of Chemistry, Wichita State University, Wichita, Kansas 67260, United States

[‡]Department of Diagnostic Medicine and Pathobiology, College of Veterinary Medicine, Kansas State University, Manhattan, Kansas 66506, United States

[§]Protein Structure Laboratory, The University of Kansas, Lawrence, Kansas 66047, United States

[||]LiS Consulting, Lawrence, Kansas 66046, United States

[⊥]IMCA-CAT, Hauptman-Woodward Medical Research Institute, APS Argonne National Laboratory, Argonne, Illinois 60439, United States

Ⓢ *Supporting Information*

ABSTRACT: Human noroviruses are the primary causative agents of acute gastroenteritis and a pressing public health burden worldwide. There are currently no vaccines or small molecule therapeutics available for the treatment or prophylaxis of norovirus infections. Norovirus 3CL protease plays a vital role in viral replication by generating structural and nonstructural proteins via the cleavage of the viral polyprotein. Thus, molecules that inhibit the viral protease may have potential therapeutic value. We describe herein the structure-based design, synthesis, and in vitro and cell-based evaluation of the first class of oxadiazole-based, permeable macrocyclic inhibitors of norovirus 3CL protease.
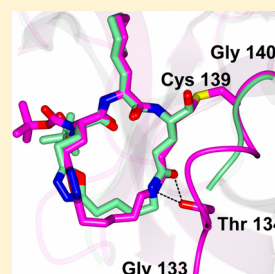
INTRODUCTION

Human noroviruses belong to the genus *Norovirus* in the family Caliciviridae.[1] They are the primary cause of sporadic and epidemic nonbacterial gastroenteritis outbreaks worldwide.[2−5] Norovirus infection is associated with high morbidity among the elderly and young, as well as immunocompromised patients.[6] The mortality rate among children in developing countries is estimated to exceed 200 000 annually.[7] Of the six norovirus genogroups (GI−VI), GI and GII are associated with human infections, with the GII.4 cluster accounting for 70−80% of norovirus outbreaks worldwide.[8] Devising prophylactic and/or therapeutic interventions for norovirus infection presents a challenge due to the high transmissibility, genetic diversity, environmental stability, and prolonged virus shedding displayed by noroviruses.[9,10] Furthermore, human noroviruses do not robustly grow in cell culture and only low levels of human norovirus are reported to grow in human B cells.[11] Lastly, there is currently no optimal animal model of the disease; consequently, many aspects of norovirus biology and pathogenesis are poorly understood.[12]

The norovirus RNA genome (7.4−7.7 kb) is a positive-sense single stranded genome comprising three open reading frames (ORF1−3) of which ORF1 encodes a 200 kDa polyprotein that is proteolytically cleaved to generate at least six nonstructural proteins: p48, RNA helicase/NTPase, p22, VPg, 3C-like protease (3CLpro), and RNA-dependent RNA polymerase (RdRp).[1,13] ORF2 and ORF3 encode the norovirus capsid (VP2) and a small basic protein (VP1), respectively. Processing of the polyprotein is effected by the norovirus 3CLpro, a cysteine protease having a chymotrypsin-like fold, an extended binding cleft, and a Cys-His-Glu catalytic triad.[14−16] The preferred substrate recognition sequence for 3CLpro is −F/Y-X-L-Q-G/A- corresponding to −P_4-P_3-P_2-P_1-P_1'-,[17] where the P_1 Gln residue determines the primary substrate specificity of the enzyme and X is H, Q, or E.[18−20] The S_3 subsite displays a degree of plasticity and, therefore, can accommodate a P_3 Gln, His, or Glu. Because processing of the polyprotein by 3CLpro is essential for viral replication, inhibition of 3CLpro is envisaged to be a fruitful avenue of investigation for the discovery of norovirus-specific antivirals, an approach that has been successfully used in the discovery of therapeutics for other viral diseases.[21,22] We have recently described an array of inhibitors of 3CLpro,[23−27] including the demonstration of in vivo efficacy by a dipeptidyl inhibitor using a murine norovirus model.[28] We report herein the results of structural, biochemical, and antiviral studies of a novel series of oxadiazole-based cell permeable macrocyclic inhibitors (I) (Figure 1) of norovirus 3CLpro.
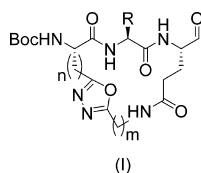
Figure 1. General structure of macrocyclic inhibitor (I).

■ RESULTS AND DISCUSSION

Inhibitor Design Rationale. There are several disadvantages associated with peptide-derived drugs, including high conformational flexibility, susceptibility to proteolytic degradation, poor membrane permeability, and low oral bioavailability.[29,30] These shortcomings are frequently mitigated through depeptitization. An effective way of depeptitizing a linear peptide is through macrocyclization.[31−34] The preorganization and structural rigidity that characterize macrocyclic inhibitors frequently enhance pharmacological activity by reducing the entropic penalty associated with binding and, furthermore, increase proteolytic stability.[34] The effect of macrocyclization on cellular permeability and oral bioavailability is less predictable; however, these parameters are expected to be augmented when a macrocycle can engage in intramolecular hydrogen bonding.[35,36] On the basis of these considerations, we hypothesized that tethering of the P_1 Gln residue, the preferred primary substrate specificity residue of norovirus 3CLpro, with the P_3 residue side chain in an appropriate linear peptide using a 1,3,4-oxadiazole linker would yield a macrocyclic scaffold (I) (Figure 1) potentially capable of participating in intramolecular hydrogen bonding via the ring oxygen or nitrogen atoms, depending on the orientation assumed by the heterocyclic ring. Additional design considerations included ensuring that the ring size of the macrocycle would be optimal in terms of allowing the macrocycle to assume a β-strand conformation, a structural motif recognized by proteases.[37,38] This is of paramount importance, since a β-strand conformation would allow proper docking/positioning of the inhibitor to the active site which, in turn, would orient correctly the side chains of the P_1 and P_2 residues, thereby maximizing hydrogen bonding and hydrophobic binding interactions. Lastly, the length of the linker and the position of the heterocyclic ring were also anticipated to influence permeability and potency by impacting the conformation of the macrocycle (vide infra).

Chemistry. A convergent approach was used in the synthesis of inhibitors **15−22** (Table 1). Thus, fragments **4a−f** and **6** were first assembled as illustrated in Scheme 1. Fragments **4a−f** were synthesized by coupling an appropriate Z-protected carboxylic acid with *tert*-butyl carbazate using EDCI to yield the Boc-protected hydrazides **1a−e**. The Boc protective group was removed via treatment with dry HCl/dioxane, and the resulting hydrazine was coupled to (L)-Boc-glutamic acid α-methyl ester using EDCI/HOBt/DIEA/DMF to yield hydrazides **2a−f**. Reaction with *p*-toluenesulfonyl chloride/DIEA in dry CH_3CN yielded 1,3,4-oxadiazole derivatives[39] **3a−f** which were hydrolyzed with LiOH in aqueous THF to yield the corresponding acids **4a−f**. Fragment **6** was readily prepared via the esterification of commercially available (L)-Boc-Glu-(OBzl)-OH with CH_3I/NaHCO_3/DMF, followed by removal of the Boc-group to yield **5**, which was then coupled to (L)-Boc-Leu using EDCI/HOBt/DIEA/DMF to form fragment **6**. Coupling of fragments **4a−f** and **6** generated leucine-substituted intermediates **7a−c** and **7e** (Scheme 2). The corresponding cyclohexylalanine-substituted compounds **7d** and **7f−h** were prepared by coupling compounds **4a−f** to (L)-cyclohexylalanine methyl ester to give esters **13a−d** which were hydrolyzed to the corresponding carboxylic acids **14a−d** (Scheme 3). Coupling of the acids with (L)-Glu(OBzl) methyl ester yielded compounds **7d** and **7f−h**. Treatment of compounds **7a−h** with H_2/Pd−C furnished acyclic precursors **8a−h**. Subsequent macrolactamization[40] yielded compounds **9a−h** which, upon reduction with lithium borohydride, generated the corresponding alcohols **10a−h**. Oxidation to aldehydes **15−22** was accomplished using Dess−Martin periodinane, and the synthesized compounds are listed in Table 1.

Biochemical Studies. The inhibitory activity of compounds **15−22** toward NV 3CLpro, as well as their antinorovirus activity in the NV replicon harboring cells established in Huh-7 cells, was determined as previously described,[26,28,41] and the results are tabulated in Table 1. A graphical dose-dependent inhibition of NV RNA replication by compound **21** is shown in Figure 2. The screening results shown in Table 1 indicate that (a) in a comparison of compounds **15**, **16**, and **22** versus compounds **17−21**, it is clearly evident that ring size has a profound impact on inhibitory activity and cellular permeability in this series of compounds; (b) with the exception of compound **22**, the rest of the inhibitors were relatively well-permeable to cells and several inhibitors displayed single digit 50% inhibitory

Table 1. Activity of Compounds 15−22 against NV 3CL Protease and Norovirus in the Cell-Based Replicon System[a]

compd	R	n	m	ring size	NV 3CLpro, IC_{50} (μM)	NV (replicon cells) EC_{50} (μM)	EC_{90} (μM)	MNV, EC_{50} (μM)	CC_{50} (μM)
15	Leu	1	1	16	>100	19.4 ± 10.8	>100	>100	>100
16	Leu	1	2	17	34.3 ± 6.9	18.1 ± 8.3	72.7 ± 5.6	>100	>100
17	Leu	2	2	18	15.3 ± 4.5	2.5 ± 1.5	23.4 ± 8.5	9.8 ± 3.3	>100
18	Cha	2	2	18	14.5 ± 3.8	5.1 ± 2.9	38.2 ± 5.2	19.9 ± 2.2	>100
19	Leu	2	3	19	21.3 ± 4.3	5.9 ± 4.5	30.5 ± 3.1	11.1 ± 3.6	>100
20	Cha	2	3	19	45.1 ± 4.6	9.4 ± 5.7	73.3 ± 4.5	>100	>100
21	Cha	2	4	20	18.5 ± 5.7	6.5 ± 2.7	18.2 ± 2.1	10.9 ± 2.3	>100
22	Cha	2	5	21	8.6 ± 3.7	51.2 ± 19.8	>100	>100	>100

[a]3CLpro, 3CL protease; IC_{50}, 50% inhibitory concentration determined by the enzyme assay; EC_{50} and EC_{90}, 50% or 90% effective concentration determined by cell-based assays, respectively; CC_{50}, 50% cytotoxic concentration in cell-based assays. Mean and the standard deviation of the mean are shown for EC_{50} and EC_{90} values.
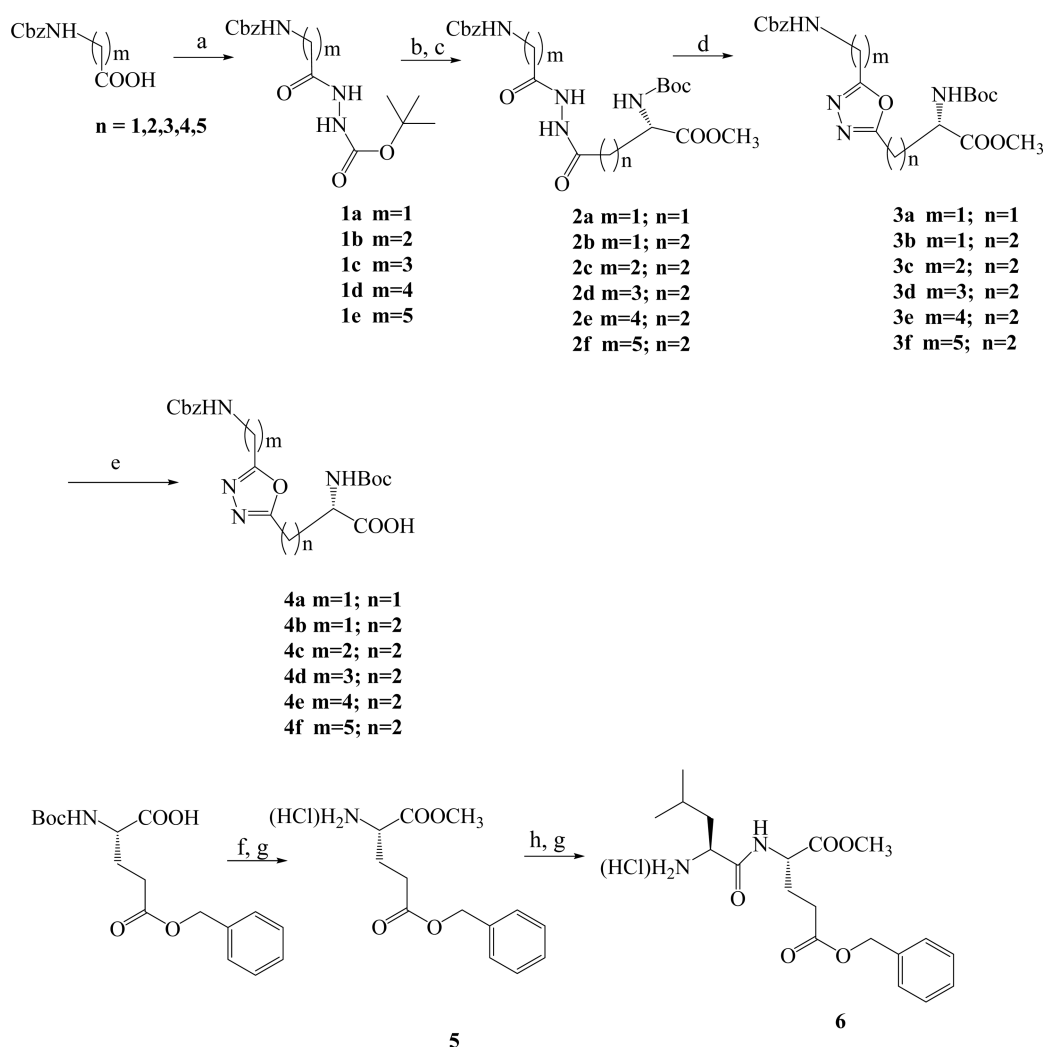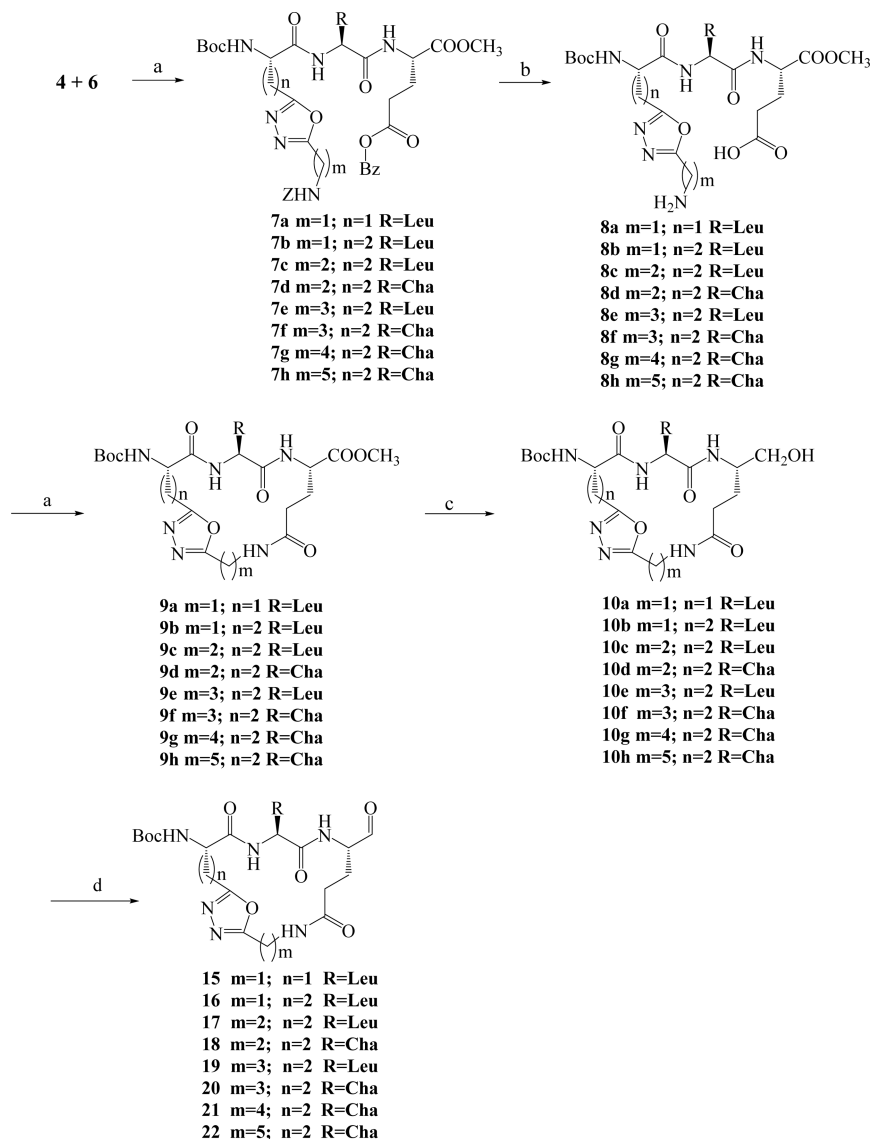
Scheme 1[a]

[a](a) *tert*-Butyl carbazate, EDCI; (b) HCl, dioxane, DCM; (c) (L)Boc-L-Glu-OMe, EDCI, HOBt, DIEA, DMF; (d) TsCI, DIEA: (e) LiOH, H₂O, THF; (f) NaHCO₃, CH₃I, DMF; (g) HCl, dioxanc; (h) Boc-L-Leu-OH, EDCI, HOBt, DIEA, DMF.

concentration (EC$_{50}$) values in cell based assays (both NV and murine norovirus-1 (MNV-1)); and (c) in contrast to acyclic dipeptidyl transition state inhibitors where the substitution of a P2 Leu residue by a P2 Cha residue results in significant improvement in both IC$_{50}$ and EC$_{50}$ values,[28] the presence of Cha at P2 did not markedly change potency (compounds **17** and **18**; compounds **19** and **20**), suggesting that a fruitful strategy for further optimization of potency may necessitate structural modifications in the "cap". In addition, the EC$_{50}$ values against NV and MNV-1 in cell culture were well correlated (Table 1), suggesting the potency (and permeability) of each compound was consistent against multiple noroviruses.

X-ray Crystallographic Studies. In order to establish the precise mechanism of action of inhibitor (I), illuminate the conformation of (I) and the orientation of the linker, as well as obtain structural information that can be used to guide the optimization of pharmacological activity, high resolution X-ray crystal structures of inhibitors **21** and **22** with NV 3CLpro were determined. Examination of the active site revealed the presence of prominent electron density in subunit A consistent with inhibitors **21** and **22** covalently bound to Cys 139 and the cyclohexyl alanine side chain nestled into the hydrophobic S$_2$

subsite[17] (Figure 3). However, for inhibitor **21**, the majority of the macrocycle was disordered and could not be modeled. This disorder was consistently observed from approximately 10 X-ray diffraction data sets obtained for this complex. A surface representation of NV 3CLpro, colored by residue type, with inhibitor **22** is shown in Figure 4.

The hydrogen-bonding interactions between NV 3CLpro and inhibitors **21** and **22** are shown in Figure 5 and include multiple hydrogen bonds between Ala160, Gln 110, and Ala158 and the inhibitor backbone which serve to correctly position the inhibitor in the active site cleft. Critical hydrogen bonds involving the P1 Gln side chain and the His157 and Thr134 residues are also clearly evident for inhibitor **22**. However, hydrogen bonding to Thr134 was not observed for the complex with inhibitor **21** due to disorder of the residues between Leu132 and Gly137. These binding interactions, as well as the flexible backbone of the T123-G133 loop, are postulated to play a critical role in enzyme recognition.[42] The lack of cellular permeability of inhibitor **22** is supported by the absence of any intramolecular hydrogen bonds with the oxadiazole ring; however, permeability involves the interplay of many factors besides intramolecular hydrogen bonding. Notably, interactions
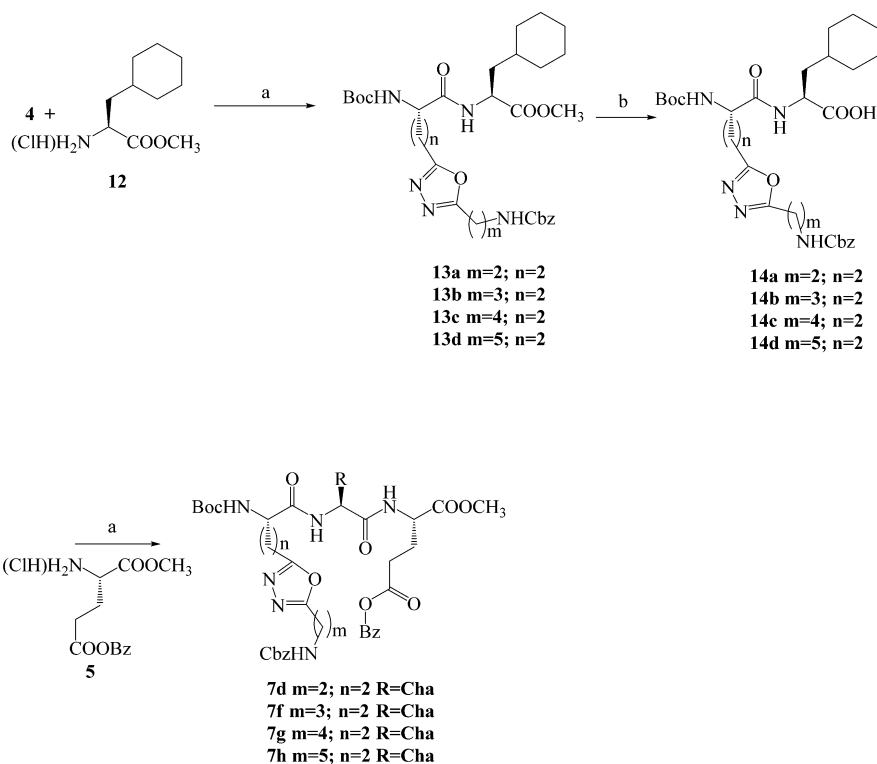
Scheme 2[a]

7a m=1; n=1 R=Leu
7b m=1; n=2 R=Leu
7c m=2; n=2 R=Leu
7d m=2; n=2 R=Cha
7e m=3; n=2 R=Leu
7f m=3; n=2 R=Cha
7g m=4; n=2 R=Cha
7h m=5; n=2 R=Cha

8a m=1; n=1 R=Leu
8b m=1; n=2 R=Leu
8c m=2; n=2 R=Leu
8d m=2; n=2 R=Cha
8e m=3; n=2 R=Leu
8f m=3; n=2 R=Cha
8g m=4; n=2 R=Cha
8h m=5; n=2 R=Cha

9a m=1; n=1 R=Leu
9b m=1; n=2 R=Leu
9c m=2; n=2 R=Leu
9d m=2; n=2 R=Cha
9e m=3; n=2 R=Leu
9f m=3; n=2 R=Cha
9g m=4; n=2 R=Cha
9h m=5; n=2 R=Cha

10a m=1; n=1 R=Leu
10b m=1; n=2 R=Leu
10c m=2; n=2 R=Leu
10d m=2; n=2 R=Cha
10e m=3; n=2 R=Leu
10f m=3; n=2 R=Cha
10g m=4; n=2 R=Cha
10h m=5; n=2 R=Cha

15 m=1; n=1 R=Leu
16 m=1; n=2 R=Leu
17 m=2; n=2 R=Leu
18 m=2; n=2 R=Cha
19 m=3; n=2 R=Leu
20 m=3; n=2 R=Cha
21 m=4; n=2 R=Cha
22 m=5; n=2 R=Cha

[a](a) EDCI, HOBT, DIEA, DMF; (b) H$_2$, Pd−C; (c) LiBH$_4$, THF; (d) Dess−Martin pcriodinane, DCM.

between inhibitor **21** and Thr134 were not observed, since the loop of NV 3CLpro spanning Gly133-Pro136 was consistently disordered. Thus, it seems that the macrocycle ring size may play a role in forming optimal hydrogen bond interactions with NV 3CLpro. Surprisingly, decreasing the macrocycle ring from 21 atoms (inhibitor **22**) to 20 atoms (inhibitor **21**) results in more disorder of the inhibitor and nearby residues of NV 3CLpro. In order to gain insight and understanding into the structural determinants that impact potency and cellular permeability, herculean efforts were expended in obtaining high resolution X-ray crystal structures of permeable inhibitors **18−20**, albeit without success. Although crystals were obtained for NV 3CLpro cocrystallized with inhibitors **18−20**, these samples only yielded weak X-ray diffraction properties even after optimization of the crystallization conditions. Finally, the crystallographic data indicate that the oxadiazole-based macrocyclic inhibitors weaken all H-bonding prospects for this pharmacophore element.

In an effort to correlate the crystal structures with the data provided in Table 1, the structures of NV 3CLpro were superimposed using secondary structure matching with GESAMT.[43] Not surprising, the overall structures of the NV 3CLpro were very similar to an rmsd of 0.54 Å between Cα atoms (158 residues). In order to conduct a more direct analysis of the inhibitors, the disordered portion of the macrocycle for inhibitor **21** was modeled in an idealized position and compared with inhibitor **22** (Figure 6). Notably, the shorter ring size of inhibitor **21** appears to move the inhibitor slightly away from the loop containing Thr134 which precludes formation of a hydrogen bond and disorder of residues Gly133-Pro136 in the nearby loop. However, inhibitor **22** is able to stabilize this loop region by formation of a hydrogen bond with Thr134 due to the larger ring size. This perhaps explains the observed difference in the IC$_{50}$ values (Table 1), as inhibitor **22** is able to form an extra hydrogen bond relative to the other inhibitors. Further shortening of the macrocycle ring size (inhibitors **15−20**) would likely move the inhibitor further away from Thr134 and prevent formation of hydrogen bonds with the loop and result in disorder of these residues. This may also explain why the crystals obtained with

Scheme 3[a]

13a m=2; n=2
13b m=3; n=2
13c m=4; n=2
13d m=5; n=2

14a m=2; n=2
14b m=3; n=2
14c m=4; n=2
14d m=5; n=2

7d m=2; n=2 R=Cha
7f m=3; n=2 R=Cha
7g m=4; n=2 R=Cha
7h m=5; n=2 R=Cha

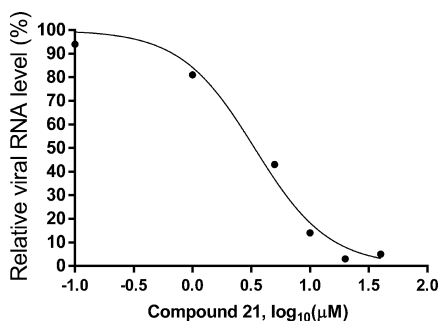[a](a) EDCI, HOBT, DIEA, DMF; (b) 1 M LiOH, H_2O, THF.

Figure 2. Dose-dependent inhibition of NV RNA levels by compound **21**. Various concentrations of compound **21** (0.1−40 μM) were incubated in NV replicon cells for 48 h, and NV RNA levels were measured by quantitative real-time RT-PCR.

Figure 3. $F_o − F_c$ map (green mesh) contoured at 3σ and $2F_o − F_c$ map (blue mesh) contoured at 1σ for of macrocyclic inhibitors (A) **22** and (B) **21** covalently bound to the catalytic cysteine residue (Cys139) of NV 3CLpro.

inhibitors **18−20** produced poor diffraction, as the dynamic conformations of the nearby loop could potentially prevent formation of well-ordered crystals. Conversely, the shorter macrocycle ring size appears to be more conducive to permeability, although binding to the NV 3CLpro target is slightly weakened.

CONCLUSIONS

There is currently a dire need for the development of norovirus-specific therapeutics and prophylactics for the management of norovirus infections. The studies described herein disclose the structure-based design of the first series of oxadiazole-based permeable macrocyclic inhibitors of norovirus 3CL protease. Insights gained from these studies have laid a solid foundation for conducting further preclinical studies focused on the optimization of potency and pharmacokinetics.
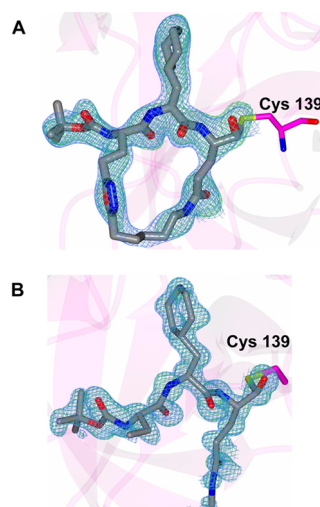
EXPERIMENTAL SECTION

General. Reagents and dry solvents were purchased from various chemical suppliers (Aldrich, Acros Organics, Chem-Impex, TCI America, Oakwood Chemicals, Bachem, and Fisher) and were used as obtained. Silica gel (230−450 mesh) used for flash chromatography was purchased from Sorbent Technologies (Atlanta, GA). Thin layer chromatography was performed using Analtech silica gel plates. The ^1H spectra were recorded in $CDCl_3$ or DMSO-d_6 on a Varian XL-400 NMR spectrometer. High resolution mass spectrometry (HRMS) experiments were performed at the University of Kansas Mass
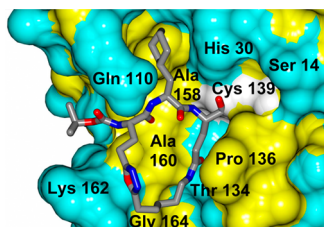
Figure 4. Surface representation of inhibitor **22** bound to NV 3CLpro with neighboring residues colored yellow (nonpolar), cyan (polar), and white (weakly polar). The P2 cyclohexylalanine side chain is snugly nestled into the hydrophobic S$_2$ subsite.
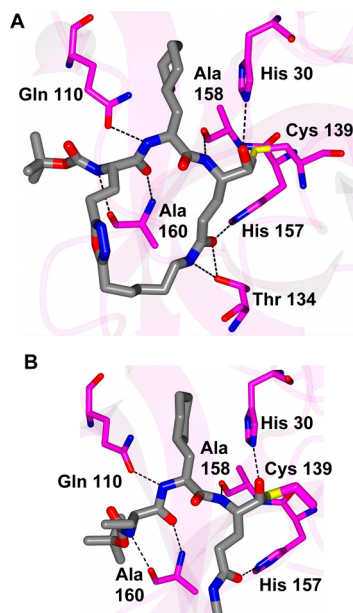

Figure 5. Hydrogen bonding interactions represented as dashed lines between NV 3CLpro and inhibitors (A) **22** and (B) **21**.
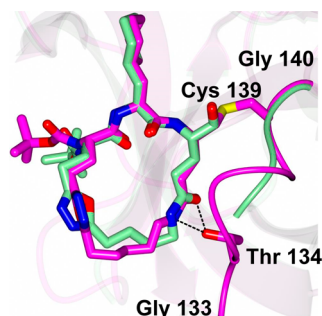

Figure 6. Superposition of NV 3CLpro complexes with inhibitors **21** (green) and **22** (magenta). The disordered portion in inhibitor **21** was modeled in an idealized geometry for comparison with inhibitor **22**.

Spectrometry lab using an LCT Premier mass spectrometer (Waters, Milford, MA) equipped with a time-of-flight mass analyzer and an electrospray ion source. Visualization was accomplished using UV light and/or iodine. Reverse phase HPLC was utilized to determine the purity of the final compounds (>95% purity).

Peptide Coupling Reactions. Synthesis of Compounds 1a–e. General Procedure. To a stirred solution of N-protected amino acid derivative (112 mmol) in dry CH$_2$Cl$_2$ (400 mL) was added EDCI (135 mmol), and the reaction mixture was stirred for 30 min at ambient temperature. *t*-Boc hydrazide (196 mmol) was added, and the reaction mixture was stirred for 18 h at room temperature. The

solution was washed with 5% aqueous HCl (2 × 100 mL), saturated NaHCO$_3$ (2 × 100 mL), and brine (100 mL). The organic phase was dried over anhydrous Na$_2$SO$_4$, filtered, and concentrated to yield the desired compounds.

***tert*-Butyl 2-(((Benzyloxy)carbonyl)glycyl)hydrazine-1-carboxylate (1a).** Yield (80%), mp 49–52 °C. ^{1}H NMR (400 MHz, CDCl$_3$) δ 1.37–1.49 (s, 9 H), 3.89 (br s, 2 H), 5.03–5.14 (s, 2 H), 7.25–7.37 (m, 5 H), 7.39–7.48 (m, 2 H). HRMS (ESI) calcd for C$_{15}$H$_{21}$N$_3$O$_5$Na, [M + Na]$^+$: 346.1379. Found: 346.1381.

***tert*-Butyl 2-(3-(((Benzyloxy)carbonyl)amino)propanoyl)-hydrazine-1-carboxylate (1b).** Yield (78%), mp 139–141 °C. ^{1}H NMR (400 MHz, CDCl$_3$): δ 1.41–1.53 (s, 9 H), 2.41–2.47 (m, 2 H), 3.45–3.55 (m, 2 H), 5.05–5.12 (s, 2 H), 6.50–6.58 (s, 1 H), 7.25–7.38 (m, 5 H), 7.63 (br s, 1 H). HRMS (ESI) calcd for C$_{16}$H$_{23}$N$_3$O$_5$Na, [M + Na]$^+$: 360.1535. Found: 360.1533.

***tert*-Butyl 2-(4-(((Benzyloxy)carbonyl)amino)butanoyl)-hydrazine-1-carboxylate (1c).** Oil, yield (80%). ^{1}H NMR (400 MHz, CDCl$_3$): δ 1.45 (s, 9 H), 1.80–1.92 (m, 5 H), 2.26 (t, J = 7.02 Hz, 3 H), 3.19–3.31 (m, 4 H), 5.05–5.17 (s, 2 H), 5.28–5.39 (m, 1 H), 6.70 (br s, 1 H), 7.26–7.39 (m, 5 H), 8.24–8.35 (m, 1 H). HRMS (ESI) calcd for C$_{17}$H$_{26}$N$_3$O$_5$ [M + H]$^+$: 352.1872. Found: 352.1874.

***tert*-Butyl 2-(5-(((Benzyloxy)carbonyl)amino)pentanoyl)-hydrazine-1-carboxylate (1d).** Oil, yield (83%). ^{1}H NMR (400 MHz, CDCl$_3$) δ 1.42–1.47 (s, 9 H), 1.48–1.56 (m, 2 H), 1.59–1.71 (m, 2 H), 2.16–2.27 (m, 2 H), 3.17 (q, J = 6.64 Hz, 2 H), 5.07 (s, 2 H), 5.22–5.35 (m, 1 H), 7.26–7.39 (m, 5 H). HRMS (ESI) calcd for C$_{18}$H$_{27}$N$_3$O$_5$Na, [M + Na]$^+$: 388.1848. Found: 388.1845.

***tert*-Butyl 2-(6-(((Benzyloxy)carbonyl)amino)hexanoyl)-hydrazine-1-carboxylate (1e).** Oil, yield (83%). ^{1}H NMR (400 MHz, CDCl$_3$) δ 1.33–1.42 (m, 2 H), 1.45 (s, 9 H), 1.59–1.72 (m, 2 H), 2.17–2.27 (m, 2 H), 2.41–2.53 (m, 2 H), 3.13–3.24 (m, 2 H), 3.36–3.47 (m, 1 H), 5.03–5.15 (m, 2 H), 7.26–7.39 (m, 5 H). HRMS (ESI) calcd for C$_{19}$H$_{30}$N$_3$O$_5$, [M + H]$^+$: 380.2185. Found: 380.2182.

Synthesis of Compounds 2a–f. General Procedure. To a solution of (L)-Boc-Glu-OMe (88.5 mmol) in dry DMF (210 mL) were added EDCI (22.05 g, 115.05 mmol, 1.3 equiv), HOBt (17.73 g, 115.05 mmol, 1.3 equiv), and the mixture was stirred for 30 min at room temperature. In a separate flask, a solution of deprotected compounds 1a–e (24.22 g, 88.5 mmol) in dry DMF (250 mL) cooled to 0–5 °C was treated with diisopropylethylamine (4.75 g, 354 mmol, 4.0 equiv). After the solution was stirred for 30 min, it was added to the solution above and the reaction mixture was stirred for 16 h while monitoring the reaction by TLC. The solvent was removed in vacuo, and the residue was partitioned between ethyl acetate (500 mL) and 5% aqueous HCl (2 × 150 mL). The layers were separated, and the organic layer was further washed with saturated aqueous NaHCO$_3$ (2 × 150 mL), followed by saturated NaCl (150 mL). The organic layer was dried over anhydrous Na$_2$SO$_4$, filtered, and concentrated to yield the desired compounds.

Methyl N^4-(2-(((Benzyloxy)carbonyl)amino)acetamido)-N^2-(*tert*-butoxycarbonyl)-L-asparaginate (2a). Yield (82%), mp 84–87 °C. ^{1}H NMR (400 MHz, CDCl$_3$): δ 1.36–1.48 (s, 9 H), 2.75–2.82 (m, 1 H), 2.84–2.88 (m, 1 H), 3.65–3.77 (s, 3 H), 3.90–3.98 (s, 2 H), 4.08–4.15 (m, 1 H), 4.57 (ddd, J = 9.52, 5.05, 4.86 Hz, 2 H), 5.05–5.15 (s, 2 H), 5.83 (d, J = 8.69 Hz, 1 H), 5.97 (br s, 1 H), 7.26–7.38 (m, 5 H). HRMS (ESI) calcd for C$_{20}$H$_{29}$N$_4$O$_8$, [M + H]$^+$: 453.1985. Found: 453.1983.

Methyl N^5-(2-(((Benzyloxy)carbonyl)amino)acetamido)-N^2-(*tert*-butoxycarbonyl)-L-glutaminate (2b). Yield (88%), mp 85–88 °C. ^{1}H NMR (400 MHz, CDCl$_3$) δ 1.36–1.48 (s, 9 H), 1.87–1.98 (t, 2 H), 2.11–2.23 (m, 2 H), 3.68–3.79 (s, 3 H), 3.96–4.03 (s, 2 H), 4.34–4.46 (m, 1 H), 5.06–5.18 (s, 1 H), 5.10 (s, 2 H), 5.44–5.57 (m, 1 H), 5.94 (br s, 1 H), 7.26–7.38 (m, 5 H), 9.21 (br s, 1 H). HRMS (ESI) calcd for C$_{21}$H$_{31}$N$_4$O$_8$, [M + H]$^+$: 467.2142. Found: 467.2143.

Methyl N^5-(3-(((Benzyloxy)carbonyl)amino)propanamido)-N^2-(*tert*-butoxycarbonyl)-L-glutaminate (2c). Yield (90%), mp 98–101 °C. ^{1}H NMR (400 MHz, DMSO-d_6) δ 1.35–1.43 (s, 9 H), 1.75–1.87 (m, 2 H), 2.18–2.20 (t, 2H), 2.77–2.90 (m, 2 H), 3.05–3.14 (m, 2 H), 3.59–3.67 (s, 3 H), 4.03 (d, J = 7.13 Hz, 1 H), 4.98–5.06 (s, 2 H), 7.29–7.42 (m, 5 H). HRMS (ESI) calcd for C$_{22}$H$_{33}$N$_4$O$_8$, [M + H]$^+$: 481.2298. Found: 481.2306.

Table 2. Crystallographic Data for NV 3CLpro:21 and NV 3CLpro:22 Complexes

	NV 3CLpro:**21**	NV 3CLpro:**22**
	Data Collection	
unit-cell parameter	a = 65.17 Å, b = 41.18 Å, c = 61.68 Å, β = 109.4°	a = 37.69 Å, b = 67.11 Å, c = 127.47 Å
space group	C2	P2$_1$2$_1$2$_1$
resolution (Å)[a]	34.21−1.00 (1.02−1.00)	42.49−2.35 (2.43−2.35)
wavelength (Å)	1.0000	1.0000
temp (K)	100	100
observed reflections	261 523	91 527
unique reflections	82 788	14 146
$\langle I/\sigma(I) \rangle$[a]	12.1 (1.9)	9.9 (2.1)
completeness (%)[a]	99.5 (90.7)	100 (100)
multiplicity[a]	3.2 (2.2)	6.5 (6.4)
R_{merge} (%)[a,b]	4.7 (47.4)	15.1 (86.8)
R_{meas} (%)[a,d]	5.6 (60.3)	16.4 (94.5)
R_{pim} (%)[a,d]	3.0 (36.7)	6.4 (36.9)
$CC_{1/2}$[a,e]	0.994 (0.764)	0.995 (0.798)
	Refinement	
resolution (Å)[a]	32.20−1.00	35.90−2.35
reflections (working/test)[a]	78 788/3 986	13 379/712
R_{factor}/R_{free} (%)[a,c]	14.3/15.4	20.9/27.8
no. of atoms (protein/ligand/water)	1319/34/132	2336/43/55
	Model Quality	
rms deviation		
bond length (Å)	0.007	0.007
bond angle (deg)	1.033	0.918
average B-factor (Å^2)		
all atoms	16.9	34.5
protein	15.4	34.6
ligand	21.0	35.8
water	31.0	30.8
coordinate error (max likelihood) (Å)	0.07	0.31
Ramachandran plot		
most favored (%)	98.9	93.9
additionally allowed (%)	1.1	5.2

[a]Values in parentheses are for the highest resolution shell. [b]$R_{merge} = \sum_{hkl}\sum_i |I_i(hkl) - \langle I(hkl)\rangle| / \sum_{hkl}\sum_i I_i(hkl)$, where $I_i(hkl)$ is the intensity measured for the ith reflection and $\langle I(hkl)\rangle$ is the average intensity of all reflections with indices hkl. [c]$R_{factor} = \sum_{hkl} ||F_{obs}(hkl)| - |F_{calc}(hkl)|| / \sum_{hkl} |F_{obs}(hkl)|$; R_{free} is calculated in an identical manner using 5% of randomly selected reflections that were not included in the refinement. [d]R_{meas} = redundancy-independent (multiplicity-weighted) R_{merge}.[52] R_{pim} = precision-indicating (multiplicity-weighted) R_{merge}.[53,54] [e]$CC_{1/2}$ is the correlation coefficient of the mean intensities between two random half-sets of data.[55,56]

Methyl N^5-(4-(((Benzyloxy)carbonyl)amino)butanamido)-N^2-(*tert*-butoxycarbonyl)-L-glutaminate (2d). Yield (85.2%), mp 105−108 °C. ^{1}H NMR (400 MHz, CDCl$_3$) δ 1.20−1.30 (m, 1 H), 1.38−1.48 (m, 6 H), 1.38−1.48 (m, 13 H), 1.59−1.71 (m, 3 H), 1.86 (t, J = 6.57 Hz, 2 H), 1.88−1.95 (m, 1 H), 2.27−2.40 (m, 5 H), 3.26−3.31 (m, 1 H), 3.70−3.79 (m, 4 H), 5.09 (s, 2 H), 7.29−7.38 (m, 5 H). HRMS (ESI) calcd for C$_{23}$H$_{35}$N$_4$O$_8$, [M + H]$^+$: 495.2455. Found: 495.2451.

Methyl N^5-(5-(((Benzyloxy)carbonyl)amino)pentanamido)-N^2-(*tert*-butoxycarbonyl)-L-glutaminate (2e). Yield (83%), mp 116−118 °C. ^{1}H NMR (400 MHz, CDCl$_3$) δ 1.39−1.46 (m, 7 H), 1.42 (s, 8 H), 1.48−1.58 (m, 2 H), 1.61−1.73 (m, 2 H), 1.89−2.01 (m, 1 H), 2.14−2.22 (m, 1 H), 2.23−2.31 (m, 2 H), 2.33−2.40 (m, 2 H), 3.12−3.25 (m, 2 H), 3.67−3.77 (m, 2 H), 3.70 (s, 3 H), 4.35 (td, J = 8.71, 4.49 Hz, 1 H), 5.07 (s, 2 H) 5.24−5.37 (m, 1 H), 5.47−5.59 (m, 1 H), 7.26−7.37 (m, 5 H), 9.03−9.15 (m, 1 H), 9.28−9.39 (m, 1 H). HRMS (ESI) calcd for C$_{24}$H$_{37}$N$_4$O$_8$, [M + H]$^+$: 509.2611. Found: 509.2615.

Methyl N^5-(6-(((Benzyloxy)carbonyl)amino)hexanamido)-N^2-(*tert*-butoxycarbonyl)-L-glutaminate (2f). Yield (79%), mp 82−85 °C. ^{1}H NMR (400 MHz, CDCl$_3$) δ 1.31−1.39 (m, 2 H), 1.40−1.53 (m, 15 H), 1.59−1.70 (m, 2 H), 1.88−2.00 (m, 1 H), 2.15−2.27 (m, 2 H), 2.30−2.43 (m, 2 H), 3.11−3.23 (m, 2 H), 3.67−3.78 (s, 3 H), 4.28−4.39 (m, 1 H), 5.06−5.18 (m, 2 H), 5.07 (s, 2 H), 5.52 (d, J = 8.89 Hz, 1 H), 7.26−7.38 (m, 5 H), 8.96−9.08 (m, 1 H), 9.26−9.37 (m, 1 H). HRMS (ESI) calcd for C$_{25}$H$_{39}$N$_4$O$_8$, [M + H]$^+$: 523.2768. Found: 523.2767.

Synthesis of Oxadiazole Compounds 3a−f. General Procedure. To a solution of compound **2** (11.0 g, 22.89 mmol) in dry acetonitrile (275 mL) were added *p*-toluenesulfonyl chloride (13.09 g, 68.67 mmol, 3.0 equiv), DIEA (5.91 g, 45.78 mmol), and the reaction mixture was stirred for 16 h at room temperature while monitoring the reaction by TLC. The solvent was removed in vacuo, and the residue was partitioned between ethyl acetate (300 mL) and 5% aqueous HCl (2 × 100 mL). The ethyl acetate layer was further washed with saturated aqueous NaHCO$_3$ (2 × 100 mL), followed by saturated NaCl (100 mL). The organic layer was dried over anhydrous Na$_2$SO$_4$, filtered, and concentrated. The crude product was purified using flash chromatography to yield the desired oxadiazole derivatives **3a−f**.

Methyl (S)-3-(5-((((Benzyloxy)carbonyl)amino)methyl)-1,3,4-oxadiazol-2-yl)-2-((*tert*-butoxycarbonyl)amino)propanoate (3a). Oil, yield (70%). ^{1}H NMR (400 MHz, CDCl$_3$) δ 1.42 (s, 9 H), 3.30−3.42 (m, 1 H), 3.71−3.83 (m, 1 H), 3.75 (s, 3 H), 4.60 (d, J = 6.05 Hz, 1 H), 4.69−4.81 (m, 1 H), 5.15 (s, 2 H), 5.46 (t, J = 6.30 Hz, 1 H), 5.51−5.57 (m, 1 H), 7.26−7.28 (m, 1 H), 7.29−7.41 (m, 5 H). HRMS (ESI) calcd for C$_{20}$H$_{27}$N$_4$O$_7$, [M + H]$^+$: 435.1880. Found: 435.1877.

Methyl (S)-4-(5-((((Benzyloxy)carbonyl)amino)methyl)-1,3,4-oxadiazol-2-yl)-2-((tert-butoxycarbonyl)amino)butanoate (3b). Oil, yield (73%). ^{1}H NMR (400 MHz, CDCl$_3$) δ 1.44 (s, 9 H), 2.06–2.17 (m, 2 H), 2.31–2.43 (m, 2 H), 2.86–2.98 (m, 2 H), 3.75 (s, 3 H), 4.34–4.46 (m, 1 H), 4.59 (d, J = 6.00 Hz, 1 H), 5.15 (s, 2 H), 5.39–5.52 (m, 1 H), 7.29–7.40 (m, 5 H). HRMS (ESI) calcd for C$_{21}$H$_{29}$N$_4$O$_7$, [M + H]$^+$: 449.2036. Found: 449.2032.

Methyl (S)-4-(5-(2-(((Benzyloxy)carbonyl)amino)ethyl)-1,3,4-oxadiazol-2-yl)-2-((tert-butoxycarbonyl)amino)butanoate (3c). Oil, yield (75%). ^{1}H NMR (400 MHz, CDCl$_3$) δ ppm 1.43 (s, 9 H), 2.04–2.16 (m, 2 H), 2.86–2.94 (t, 2 H), 2.98–3.10 (t, 2 H), 3.62–3.69 (m, 2 H), 3.73 (s, 3 H), 4.35–4.45 (br s 1H), 5.17–5.25 (br s, 1 H), 5.67–5.72 (br s, 1 H), 5.07–5.13 (s, 2 H), 7.25–7.38 (m, 5 H). HRMS (ESI) calcd for C$_{22}$H$_{31}$N$_4$O$_7$, [M + H]$^+$: 463.2193. Found: 463.2190.

Methyl (S)-4-(5-(3-(((Benzyloxy)carbonyl)amino)propyl)-1,3,4-oxadiazol-2-yl)-2-((tert-butoxycarbonyl)amino)-butanoate (3d). Oil, yield (75%). ^{1}H NMR (400 MHz, CDCl$_3$) δ 1.38–1.49 (s, 9 H), 1.96–2.07 (m, 2 H), 2.08–2.11 (m, 2 H), 2.42 (br s, 1 H), 2.84–2.91 (m, 2 H), 2.96–3.06 (m, 2 H), 3.24–3.36 (m, 2 H), 3.74 (s, 3 H), 4.38–4.45 (m, 1H), 5.09 (s, 2 H), 5.12–5.20 (m, 1 H), 7.29–7.40 (m, 5 H). HRMS (ESI) calcd for C$_{23}$H$_{33}$N$_4$O$_7$, [M + H]$^+$: 477.2349. Found: 477.2346.

Methyl (S)-4-(5-(4-(((Benzyloxy)carbonyl)amino)butyl)-1,3,4-oxadiazol-2-yl)-2-((tert-butoxycarbonyl)amino)butanoate (3e). Oil, yield (79%), ^{1}H NMR (400 MHz, CDCl$_3$) δ ppm 1.37–1.49 (s, 9 H), 1.54–1.67 (m, 2 H), 1.77–1.89 (m, 2 H), 2.30–2.42 (m, 1 H), 2.80–2.93 (m, 4 H), 3.16–3.28 (m, 2 H), 3.74 (s, 3 H), 4.34–4.46 (m, 1 H), 4.96–5.04 (m, 1 H), 5.09 (s, 2 H), 7.27–7.39 (m, 5 H). HRMS (ESI) calcd for C$_{24}$H$_{35}$N$_4$O$_7$, [M + H]$^+$: 491.2506. Found: 491.2504.

Methyl (S)-4-(5-(5-(((Benzyloxy)carbonyl)amino)pentyl)-1,3,4-oxadiazol-2-yl)-2-((tert-butoxycarbonyl)amino)-butanoate (3f). Oil, yield (80%). ^{1}H NMR (400 MHz, CDCl$_3$) δ ppm 1.37–1.49 (s, 9 H), 1.50–1.60 (m, 2 H), 1.75–1.87 (m, 2 H), 2.81 (t, J = 7.52 Hz, 2 H), 2.87–2.95 (m, 2 H), 3.13–3.25 (m, 2 H), 3.71–3.80 (m, 2 H), 3.74 (s, 3 H), 4.36–4.46 (m, 1 H), 4.83–4.96 (m, 1 H), 5.09 (s, 2 H), 5.18–5.31 (m, 1 H), 7.27–7.39 (m, 5 H). HRMS (ESI) calcd for C$_{25}$H$_{37}$N$_4$O$_7$, [M + H]$^+$: 505.2662. Found: 505.2657.

Synthesis of Acids 4a–f. General Procedure. A solution of ester **3** (20 mmol) in THF (30 mL) was treated with 1 M LiOH in aqueous THF (40 mL). The reaction mixture was stirred for 3 h at room temperature, and the disappearance of the ester was monitored by TLC. Most of the solvent was evaporated off, and the residue was diluted with water (25 mL). The solution was acidified to pH ≈ 3 using 5% hydrochloric acid (20 mL), and the aqueous layer was extracted with ethyl acetate (3 × 100 mL). The combined organic layers were dried over anhydrous sodium sulfate, filtered, and concentrated to yield the desired compound.

(S)-3-(5-((((Benzyloxy)carbonyl)amino)methyl)-1,3,4-oxadiazol-2-yl)-2-((tert-butoxycarbonyl)amino)propanoic Acid (4a). Yield (95%), mp 78–80 °C. ^{1}H NMR (400 MHz, CDCl$_3$) δ 1.42 (s, 9 H), 3.30–3.42 (m, 1 H), 3.71–3.83 (m, 1 H), 4.60 (d, J = 6.05 Hz, 1 H), 4.69–4.81 (m, 1 H), 5.15 (s, 2 H), 5.46 (t, J = 6.30 Hz, 1 H), 5.51–5.57 (m, 1 H), 7.26–7.28 (m, 1 H), 7.29–7.41 (m, 5 H). HRMS (ESI) calcd for C$_{19}$H$_{25}$N$_4$O$_7$, [M + H]$^+$: 421.1723. Found: 421.1719.

(S)-4-(5-((((Benzyloxy)carbonyl)amino)methyl)-1,3,4-oxadiazol-2-yl)-2-((tert-butoxycarbonyl)amino)butanoic Acid (4b). Oil, yield (94%). ^{1}H NMR (400 MHz, CDCl$_3$) δ 1.44 (s, 9 H), 2.06–2.17 (m, 2 H), 2.31–2.43 (m, 2 H), 2.86–2.98 (m, 2 H), 4.34–4.46 (m, 1 H), 4.59 (d, J = 6.00 Hz, 1 H), 5.15 (s, 2 H), 5.39–5.52 (m, 1 H), 7.29–7.40 (m, 5 H). HRMS (ESI) calcd for C$_{20}$H$_{27}$N$_4$O$_7$, [M + H]$^+$: 435.1880. Found: 435.1885.

(S)-4-(5-(2-(((Benzyloxy)carbonyl)amino)ethyl)-1,3,4-oxadiazol-2-yl)-2-((tert-butoxycarbonyl)amino)butanoic Acid (4c). Yield (94%), mp 96–98 °C. ^{1}H NMR (400 MHz, CDCl$_3$) δ ppm 1.43 (s, 9 H), 2.04–2.16 (m, 2 H), 2.86–2.94 (t, 2 H), 2.98–3.10 (t, 2 H), 3.62–3.69 (m, 2 H), 4.35–4.45 (br s, 1H), 5.17–5.25 (br. s, 1 H), 5.67–5.72 (br s, 1 H), 5.07–5.13 (s, 2 H), 7.25–7.38 (m, 5 H).

HRMS (ESI) calcd for C$_{21}$H$_{29}$N$_4$O$_7$, [M + H]$^+$: 449.2036. Found: 449.2047.

(S)-4-(5-(3-(((Benzyloxy)carbonyl)amino)propyl)-1,3,4-oxadiazol-2-yl)-2-((tert-butoxycarbonyl)amino)butanoic Acid (4d). Oil, yield (96%). ^{1}H NMR (400 MHz, CDCl$_3$) δ 1.38–1.49 (s, 9 H), 1.96–2.07 (m, 4 H), 2.08–2.11 (m, 2 H), 2.35–2.41 (m, 1 H), 2.42 (br s, 1 H), 2.84–2.91 (m, 2 H), 2.96–3.06 (m, 2 H), 3.24–3.36 (m, 2 H), 4.38–4.45 (m, 1H), 5.09 (s, 2 H), 5.12–5.20 (m, 1 H), 7.29–7.40 (m, 5 H). HRMS (ESI) calcd for C$_{22}$H$_{30}$N$_4$O$_7$Na, [M + Na]$^+$: 485.2012. Found: 485.2017.

(S)-4-(5-(4-(((Benzyloxy)carbonyl)amino)butyl)-1,3,4-oxadiazol-2-yl)-2-((tert-butoxycarbonyl)amino)butanoic Acid (4e). Oil, yield (95%). ^{1}H NMR (400 MHz, CDCl$_3$) δ 1.38–1.50 (s, 9 H), 1.55–1.64 (m, 2 H), 1.75–1.84 (m, 2 H), 2.22 (dd, J = 7.37, 6.88 Hz, 2 H), 2.42 (d, J = 7.13 Hz, 1 H), 2.79–2.91 (m, 2 H), 2.97 (br s, 1 H), 2.99 (t, J = 7.79 Hz, 2 H), 3.18–3.27 (m, 2 H), 5.08 (br s, 2 H), 5.44–5.51 (m, 1 H), 7.26–7.38 (m, 5 H). HRMS (ESI) calcd for C$_{23}$H$_{33}$N$_4$O$_7$, [M + H]$^+$: 477.2349. Found: 477.2340.

(S)-4-(5-(5-(((Benzyloxy)carbonyl)amino)pentyl)-1,3,4-oxadiazol-2-yl)-2-((tert-butoxycarbonyl)amino)butanoic Acid (4f). Oil, yield (95%). ^{1}H NMR (400 MHz, CDCl$_3$) δ 1.37–1.49 (s, 9 H), 1.50–1.60 (m, 2 H), 1.75–1.87 (m, 2 H), 2.81 (t, J = 7.52 Hz, 2 H), 2.87–2.95 (m, 2 H), 3.13–3.25 (m, 2 H), 3.71–3.80 (m, 2 H), 4.36–4.46 (m, 1 H), 4.83–4.96 (m, 1 H), 5.09 (s, 2 H), 5.18–5.31 (m, 1 H), 7.27–7.39 (m, 5 H). HRMS (ESI) calcd for C$_{24}$H$_{35}$N$_4$O$_7$, [M + H]$^+$: 491.2506. Found: 491.2513.

Synthesis of Amino Acid Methyl Esters 5. General Procedure. To a solution of (L)-Boc-Glu(OBzl)-OH (16.86 g, 50 mmol) in dry DMF (100 mL) was added NaHCO$_3$ (25.2 g, 300 mmol) followed by methyl iodide (14.2 g, 100 mmol). The reaction mixture was stirred for 72 h at room temperature. The progress of the reaction was monitored by TLC. The solids were filtered off, and the solvent was removed in vacuo. The residue was partitioned between ethyl acetate (250 mL) and water (2 × 75 mL). The ethyl acetate layer was washed with saturated NaCl (75 mL) and the organic layer was dried over anhydrous Na$_2$SO$_4$, filtered and concentrated to yield an oily product, which was purified by flash chromatography to yield compound **5** as a colorless oil.

5-Benzyl 1-Methyl (tert-Butoxycarbonyl)glutamate (5). Oil, yield (85%). ^{1}H NMR (400 MHz, CDCl$_3$) δ 1.36–1.49 (s, 9 H), 1.90–2.00 (m, 1 H), 2.12–2.24 (m, 2 H), 2.37–2.48 (m, 2 H), 3.66–3.75 (s, 3 H), 4.25–4.38 (m, 1 H), 5.04–5.16 (m, 1 H), 5.10 (s, 2 H), 7.28–7.40 (m, 5 H).

Synthesis of Compound 6. General Procedure. To a solution of (L)-Boc-Leu-OH (54.87 mmol) in dry DMF (100 mL) were added EDCI (12.83 g, 66.94 mmol, 1.3 equiv), HOBt (10.27 g, 66.94 mmol, 1.3 equiv), and the reaction mixture was stirred for 30 min at room temperature. In a separate flask, a solution of deprotected compound **5** (15.8 g, 54.87 mmol) in dry DMF (100 mL) cooled to 0–5 °C was treated with diisopropylethylamine (DIEA) (28.36 g, 219.48 mmol, 4.0 equiv), stirred for 30 min, and then added to the above reaction mixture. The solution was stirred for 16 h while monitoring the reaction by TLC. The solvent was removed and the residue was partitioned between ethyl acetate (300 mL) and 5% aqueous HCl (2 × 120 mL). The ethyl acetate layer was further washed with aqueous NaHCO$_3$ (2 × 120 mL), followed by saturated NaCl (120 mL). The organic layer was dried over anhydrous Na$_2$SO$_4$, filtered, and concentrated to yield a yellow oil which was purified by flash chromatography to yield an oily product which was deblocked with 4 M HCl in dioxane to yield compound **6**.

Synthesis of Compounds 7a–h. General Procedure. To a solution of compound **4** (10.0 g, 22.29 mmol) in dry DMF (100 mL) was added EDCI (5.55 g, 28.98 mmol, 1.3 equiv), and the mixture was stirred for 30 min at room temperature. In a separate flask, a solution of deprotected compound **6** (7.6 g, 22.29 mmol) in dry DMF (100 mL) cooled to 0–5 °C was treated with diisopropylethylamine (DIEA) (11.52 g, 89.16 mmol, 4.0 equiv), stirred for 30 min, and then added to the reaction mixture above. The solution was stirred for 16 h while monitoring the reaction by TLC, and the solvent was removed in vacuo. The residue was partitioned between (400 mL) and 5%

aqueous HCl (2 × 120 mL). The ethyl acetate layer was further washed with saturated aqueous NaHCO₃ (2 × 120 mL), followed by saturated NaCl (120 mL). The organic layer was dried over anhydrous Na₂SO₄, filtered, and concentrated. The crude product was purified by flash chromatography to yield the desired products.

5-Benzyl 1-Methyl ((S)-3-(5-((((Benzyloxy)carbonyl)amino)-methyl)-1,3,4-oxadiazol-2-yl)-2-((tert-butoxycarbonyl)amino)-propanoyl)-L-leucyl-L-glutamate (7a). Yield (70%), mp 80–82 °C. ^{1}H NMR (400 MHz, DMSO-d_6) δ 0.79–0.91 (m, 6 H), 1.38–1.42 (s, 9 H), 1.42–1.49 (m, 1 H), 1.57–1.68 (m, 1 H), 1.83–1.94 (m, 1 H), 1.97–2.08 (m, 1 H), 2.40–2.52 (m, 2 H), 2.98–3.11 (m, 1 H), 3.13–3.25 (m, 1 H), 3.32 (br s, 1 H), 3.55–3.65 (s, 3 H), 4.26–4.35 (s, 2 H), 4.36–4.42 (m, 1 H), 4.52–4.54 (s, 2 H), 4.99–5.12 (s, 4 H), 7.14–7.26 (m, 1 H), 7.27–7.40 (m, 10 H), 7.92–8.05 (m, 1 H), 8.26–8.38 (m, 1 H). HRMS (ESI) calcd for C₃₈H₅₁N₆O₁₁, [M + H]⁺: 767.3616. Found: 767.3612.

5-Benzyl 1-Methyl ((S)-4-(5-((((Benzyloxy)carbonyl)amino)-methyl)-1,3,4-oxadiazol-2-yl)-2-((tert-butoxycarbonyl)amino)-butanoyl)-L-leucyl-L-glutamate (7b). Yield (67%), mp 94–98 °C. ^{1}H NMR (400 MHz, CDCl₃) δ 0.86–0.98 (m, 6 H), 1.36–1.49 (s, 9 H), 1.54–1.61 (m, 1 H), 1.62–1.72 (m, 2 H), 1.95–2.07 (m, 2 H), 2.16–2.28 (m, 2 H), 2.36–2.48 (m, 2 H), 2.86–2.98 (m, 2 H), 3.65–3.76 (s, 3 H), 4.11–4.22 (m, 1 H), 4.37–4.48 (m, 1 H), 4.50–4.63 (s, 2 H), 5.07–5.19 (s, 4 H), 5.26–5.38 (m, 1 H), 5.65–5.74 (m, 1 H), 6.94–7.06 (m, 1 H), 7.28–7.39 (m, 10 H), 8.30–8.32 (d, 1 H). HRMS (ESI) calcd for C₃₉H₅₃N₆O₁₁, [M + H]⁺: 781.3772. Found: 781.3765.

5-Benzyl 1-Methyl ((S)-4-(5-(2-(((Benzyloxy)carbonyl)-amino)ethyl)-1,3,4-oxadiazol-2-yl)-2-((tert-butoxycarbonyl)-amino)butanoyl)-L-leucyl-L-glutamate (7c). Yield (79%), mp 95–97 °C. ^{1}H NMR (400 MHz, CDCl₃) δ 0.85–0.97 (m, 6 H), 1.39 (s, 9 H), 1.51–1.59 (m, 1 H), 1.61–1.71 (m, 2 H), 1.96–2.07 (m, 2 H), 2.14–2.26 (m, 2 H), 2.38–2.49 (m, 2 H), 2.87–2.96 (m, 2 H), 2.98–3.03 (m, 1 H), 3.60–3.66 (m, 2 H), 3.68–3.73 (s, 3 H), 4.09–4.19 (m, 1 H), 4.33–4.45 (m, 1 H), 4.53–4.63 (m, 1 H), 5.05–5.17 (s, 4 H), 5.3–5.4 (dd, 1H), 5.65 5.75 (dd, 1H), 7.03–7.15 (m, 1 H), 7.26–7.38 (m, 10 H), 8.22–8.30 (dd, 2 H). HRMS (ESI) calcd for C₄₀H₅₅N₆O₁₁, [M + H]⁺: 795.3929. Found: 795.3914.

5-Benzyl 1-Methyl ((S)-4-(5-(3-(((Benzyloxy)carbonyl)-amino)propyl)-1,3,4-oxadiazol-2-yl)-2-((tert-butoxycarbonyl)-amino)butanoyl)-L-leucyl-L-glutamate (7e). Yield (74%), mp 80–83 °C. ^{1}H NMR (400 MHz, CDCl₃) δ 0.86–0.99 (m, 6 H), 1.41 (s, 9 H), 1.56–1.63 (m, 1 H), 1.66–1.75 (m, 4 H), 1.80–1.91 (m, 2 H), 1.96–2.09 (m, 2 H), 2.18–2.28 (m, 2 H), 2.37–2.49 (m, 2 H), 2.51–2.62 (m, 2 H), 2.83–2.95 (m, 2 H), 3.29 (dd, J = 6.52, 0.66 Hz, 1 H), 3.69 (s, 3 H), 4.05–4.17 (m, 1 H), 4.38–4.47 (m, 1H), 4.54–4.63 (m, 1 H), 5.04–5.17 (s, 4 H), 6.21–6.22 (d, 1 H), 6.42–6.44 (d, 1 H), 7.26–7.27 (m, 1 H), 7.29–7.39 (m, 10 H), 9.10–9.12 (d, 1 H). HRMS (ESI) calcd for C₄₁H₅₇N₆O₁₁, [M + H]⁺: 809.4085. Found: 809.4081.

Hydrogenolysis of Benzyl Esters 8a–h. General Procedure. To a solution of benzyl ester 7 (12.0 g, 15.09 mmol) in methanol 120 mL (10 mL/g of ester) was added 10% palladium on carbon (0.80 g, 50 mol %), and the mixture was shaken on a Parr hydrogenator for 8 h under 40 atm of H₂ while monitoring the reaction by TLC. The reaction mixture was filtered through Celite, and the Celite bed was washed with methanol. The filtrate was concentrated under reduced pressure to yield compounds 8a–h.

(6S,9S,12S)-6-((5-(Aminomethyl)-1,3,4-oxadiazol-2-yl)-methyl)-9-isobutyl-12-(methoxycarbonyl)-2,2-dimethyl-4,7,10-trioxo-3-oxa-5,8,11-triazapentadecan-15-oic Acid (8a). Yield (95%), mp 102–104 °C. ^{1}H NMR (400 MHz, DMSO-d_6) δ 0.79–0.92 (m, 6 H), 1.36 (s, 9 H), 1.42–1.49 (m, 2 H), 1.56–1.68 (m, 1 H), 1.76–1.89 (m, 1 H), 1.90–2.02 (m, 1 H), 2.20–2.30 (m, 2 H), 3.01–3.12 (m, 1 H), 3.16–3.29 (m, 1 H), 3.56–3.68 (s, 3 H), 3.84 (s, 2 H), 4.21–4.28 (m, 1 H), 4.30–4.36 (m, 1 H), 4.37–4.43 (m, 1 H), 7.19–7.28 (m, 1 H), 7.28–7.40 (m, 1 H), 7.94–8.07 (m, 1 H), 8.32–8.44 (m, 2 H). HRMS (ESI) calcd for C₂₃H₃₉N₆O₉, [M + H]⁺: 543.2779. Found: 543.2773.

(6S,9S,12S)-6-(2-(5-(Aminomethyl)-1,3,4-oxadiazol-2-yl)-ethyl)-9-isobutyl-12-(methoxycarbonyl)-2,2-dimethyl-4,7,10-

trioxo-3-oxa-5,8,11-triazapentadecan-15-oic Acid (8b). Yield (95%), mp 106–110 °C. ^{1}H NMR (400 MHz, DMSO-d_6) δ 0.80–0.93 (d, 6 H), 1.38 (s, 9 H), 1.45 (t, J = 7.37 Hz, 2 H), 1.58–1.71 (m, 1 H), 1.75–1.84 (m, 1 H), 1.89–2.02 (m, 3 H), 2.19–2.31 (m, 3 H), 2.50 (dt, J = 3.72, 1.87 Hz, 1 H), 2.77–2.88 (m, 2 H), 3.55–3.66 (s, 3 H), 3.86 (s, 2 H), 3.94–4.06 (m, 1 H), 4.21–4.29 (m, 1 H), 4.30–4.39 (m, 1 H), 7.04–7.12 (m, 1 H), 7.90–7.97 (m, 1 H), 8.30–8.41 (m, 1 H). HRMS (ESI) calcd for C₂₄H₄₁N₆O₉, [M + H]⁺: 557.2935. Found: 557.2930.

(6S,9S,12S)-6-(2-(5-(2-Aminoethyl)-1,3,4-oxadiazol-2-yl)-ethyl)-9-(cyclohexylmethyl)-12-(methoxycarbonyl)-2,2-di-methyl-4,7,10-trioxo-3-oxa-5,8,11-triazapentadecan-15-oic Acid (8c). Yield (94%), mp 90–93 °C. ^{1}H NMR (400 MHz, CDCl₃) δ 0.83–0.95 (m, 2 H), 1.12–1.20 (m, 2 H), 1.24–1.28 (m, 1 H), 1.37–1.48 (s, 9 H), 1.61–1.74 (m, 6 H), 1.96–2.08 (t, 2 H), 2.15–2.27 (m, 2 H), 2.19 (s, 2 H), 2.36–2.49 (m, 2 H), 2.87–2.96 (m, 2 H), 2.97–3.03 (m, 1 H), 3.60–3.72 (m, 2 H), 3.60–3.72 (s, 3 H), 4.11–4.20 (m, 1 H), 4.50–4.63 (m, 2 H), 7.09–7.18 (m, 1 H), 8.2–8.3 (dd, 2 H). HRMS (ESI) calcd for C₂₅H₄₃N₆O₉, [M + H]⁺: 571.3092. Found: 571.3089.

(6S,9S,12S)-6-(2-(5-(2-Aminoethyl)-1,3,4-oxadiazol-2-yl)-ethyl)-9-(cyclohexylmethyl)-12-(methoxycarbonyl)-2,2-di-methyl-4,7,10-trioxo-3-oxa-5,8,11-triazapentadecan-15-oic Acid (8d). Yield (94%), mp 119–121 °C. ^{1}H NMR (400 MHz, DMSO-d_6) δ 0.79–0.91 (m, 2 H), 1.08–1.20 (m, 4 H), 1.32–1.43 (s, 9 H), 1.44–1.48 (m, 1 H), 1.59–1.67 (m, 4 H), 1.69–1.73 (m, 2 H), 1.87–1.96 (m, 2 H), 1.97–2.02 (m, 1 H), 2.05–2.13 (m, 2 H), 2.48–2.54 (m, 2 H), 2.76–2.86 (m, 2 H), 2.92–3.05 (m, 4 H), 3.10–3.21 (m, 1 H), 3.57–3.68 (s, 3 H), 3.96–4.08 (m, 1 H), 4.17–4.29 (m, 1 H), 4.30–4.43 (m, 1 H)m 7.03–7.14 (m, 1 H)m 7.94–8.07 (m, 1 H)m 8.39–8.46 (m, 1 H). HRMS (ESI) calcd for C₂₈H₄₇N₆O₉, [M + H]⁺: 611.3405. Found: 611.3400.

(6S,9S,12S)-6-(2-(5-(3-Aminopropyl)-1,3,4-oxadiazol-2-yl)-ethyl)-9-isobutyl-12-(methoxycarbonyl)-2,2-dimethyl-4,7,10-trioxo-3-oxa-5,8,11-triazapentadecan-15-oic Acid (8e). Yield (94%), mp 102–105 °C. ^{1}H NMR (400 MHz, CDCl₃) δ 0.86–0.97 (m, 6 H), 1.43 (s, 9 H), 1.58–1.65 (m, 1 H), 1.66–1.75 (m, 4 H), 1.83–1.93 (m, 2 H), 1.96–2.09 (m, 2 H), 2.18–2.28 (m, 2 H), 2.37–2.49 (m, 2 H), 2.51–2.62 (m, 2 H), 2.83–2.95 (m, 2 H), 3.29 (dd, J = 6.52, 0.66 Hz, 1 H), 3.69 (s, 3 H), 4.05–4.17 (m, 1 H), 4.38–4.47 (m, 1H), 4.54–4.63 (m, 1 H), 6.21–6.22 (d, 1 H), 6.42–6.44 (d, 1 H), 7.26–7.27 (m, 1 H), 9.10–9.12 (d, 1 H). HRMS (ESI) calcd for C₂₆H₄₅N₆O₉, [M + H]⁺: 585.3248. Found: 585.3244.

(6S,9S,12S)-6-(2-(5-(3-Aminopropyl)-1,3,4-oxadiazol-2-yl)-ethyl)-9-(cyclohexylmethyl)-12-(methoxycarbonyl)-2,2-di-methyl-4,7,10-trioxo-3-oxa-5,8,11-triazapentadecan-15-oic Acid (8f). Yield (96%), mp 117–120 °C. ^{1}H NMR (400 MHz, DMSO-d_6) δ 0.78–0.90 (m, 2 H), 1.08–1.19 (m, 2 H), 1.32–1.41 (m, 4 H), 1.37 (s, 9 H), 1.42–1.46 (m, 1 H), 1.59–1.71 (m, 6 H), 1.81–1.86 (m, 2 H), 1.87–1.94 (m, 2 H), 2.03–2.15 (m, 1 H), 2.21–2.29 (m, 2 H), 2.37–2.44 (m, 1 H), 2.50 (dt, J = 3.73, 1.89 Hz, 2 H), 3.16–3.22 (m, 1 H), 3.58–3.68 (s, 3 H), 3.84–3.96 (m, 1 H), 4.22–4.28 (m, 1 H), 4.29–4.41 (m, 2 H), 6.88–7,00 (m, 1 H), 7.88–8.00 (m, 1 H), 8.37–8.45 (m, 1 H). HRMS (ESI) calcd for C₂₉H₄₉N₆O₉, [M + H]⁺: 625.3561. Found: 625.3558.

(6S,9S,12S)-6-(2-(5-(4-Aminobutyl)-1,3,4-oxadiazol-2-yl)-ethyl)-9-(cyclohexylmethyl)-12-(methoxycarbonyl)-2,2-di-methyl-4,7,10-trioxo-3-oxa-5,8,11-triazapentadecan-15-oic Acid (8g). Yield (91%), mp 111–113 °C. ^{1}H NMR (400 MHz, DMSO-d_6) δ 0.79–0.91 (m, 2 H), 1.07–1.18 (m, 4 H), 1.33–1.42 (m, 4 H), 1.38 (s, 9 H), 1.44–1.47 (m, 2 H), 1.58–1.68 (m, 4 H), 1.76–1.82 (m, 3 H), 1.84–1.96 (m, 4 H), 2.18–2.30 (t, 2 H), 2.58–2.70 (t, 2 H), 2.76 (t, J = 6.41 Hz, 2 H), 3.57–3.69 (s, 3 H), 3.74–3.87 (m, 2 H), 3.91–4.04 (m, 1 H), 4.19–4.30 (m, 1 H), 4.32–4.44 (m, 1 H), 7.05–7.1 (d, 1H), 7.91–8.03 (m, 1 H), 8.41 (d, J = 7.32 Hz, 1 H). HRMS (ESI) calcd for C₃₀H₅₁N₆O₉, [M + H]⁺: 639.3718. Found: 639.3715.

(6S,9S,12S)-6-(2-(5-(4-Aminobutyl)-1,3,4-oxadiazol-2-yl)-ethyl)-9-(cyclohexylmethyl)-12-(methoxycarbonyl)-2,2-di-methyl-4,7,10-trioxo-3-oxa-5,8,11-triazapentadecan-15-oic Acid (8h). Yield (96%), mp 103–106 °C. ^{1}H NMR (400 MHz,

CDCl$_3$) δ 0.85−0.97 (m, 2 H), 1.12−1.22 (m, 2 H), 1.24−1.28 (m, 2 H), 1.36−1.46 (m, 4 H), 1.42 (s, 9 H), 1.49−1.58 (m, 2 H), 1.63−1.72 (m, 4 H), 1.74−1.76 (m, 2 H), 1.96−2.08 (m, 2 H), 2.16−2.29 (m, 2 H), 2.37−2.49 (m, 2 H), 2.76−2.83 (m, 2 H), 2.86−2.98 (m, 2 H), 3.11−3.24 (m, 2 H), 3.66−3.76 (s, 3 H), 4.0−4.15 (br s, 1H), 4.54−4.64 (m, 2 H), 7.02−7.15 (m, 1 H), 7.92−8.04 (d, 1 H), 8.45 (d, J = 7.9 Hz, 1 H). HRMS (ESI) calcd for C$_{31}$H$_{53}$N$_6$O$_9$, [M + H]$^+$: 653.3874. Found: 653.3871.

Synthesis of Macrocyclic Oxadiazole Esters 9a−h. General Procedure. To a solution of compound **8** (2.0 g, 3.5 mmol) in dry DMF (750 mL) were added EDCI (0.87 g, 4.55 mmol, 1.3 equiv), HOBt (0.7 g, 4.55 mmol, 1.3 equiv), DIEA (1.35 g, 10.5 mmol, 3.0 equiv), and the mixture was stirred for 18 h at room temperature while monitoring the reaction by TLC. The solvent was removed, and the residue was partitioned between ethyl acetate (200 mL) and 10% citric acid (2 × 50 mL). The ethyl acetate layer was further washed with saturated aqueous NaHCO$_3$ (2 × 50 mL), followed by saturated NaCl (50 mL). The organic layer was dried over anhydrous Na$_2$SO$_4$, filtered, and concentrated. The crude product was purified by flash chromatography to yield compounds **9a−h**.

Methyl (7S,10S,13S)-13-((*tert*-Butoxycarbonyl)amino)-10-isobutyl-4,9,12-trioxo-3,8,11-triaza-1(2,5)-oxadiazolacyclotetradecaphane-7-carboxylate (9a). Yield (60%), mp 160−163 °C. ^{1}H NMR (400 MHz, DMSO-d_6) δ 0.88 (dd, J = 12.52, 6.57 Hz, 6 H), 1.43 (s, 9 H), 1.59−1.70 (m, 2 H), 2.09−2.18 (m, 1 H), 2.20−2.28 (m, 1 H), 2.35−2.45 (m, 1 H), 3.12−3.21 (m, 1 H), 3.27 (dd, J = 15.01, 7.01 Hz, 1 H), 3.31−3.40 (m, 1 H), 3.56−3.69 (m, 1 H), 3.56−3.69 (s, 3 H), 4.07−4.18 (m, 1 H), 4.27−4.39 (m, 1 H), 4.39−4.50 (m, 1 H), 4.50−4.61 (m, 1 H), 4.78 (dd, J = 16.01, 7.91 Hz, 1 H), 6.17 (dd, J = 7.88, 0.12 Hz, 1 H), 7.31−7.43 (m, 1 H), 8.16−8.24 (m, 1 H), 8.27 (d, J = 8.45 Hz, 1 H). HRMS (ESI) calcd for C$_{23}$H$_{36}$N$_6$O$_8$Na, [M + Na]$^+$: 547.2492. Found: 547.2504.

Methyl (7S,10S,13S)-13-((*tert*-Butoxycarbonyl)amino)-10-isobutyl-4,9,12-trioxo-3,8,11-triaza-1(2,5)-oxadiazolacyclopentadecaphane-7-carboxylate (9b). Yield (67%), mp 177−180 °C. ^{1}H NMR (400 MHz, DMSO-d_6) δ 0.80−0.93 (m, 6 H), 1.33−1.41 (s, 9 H), 1.42−1.47 (m, 2 H), 1.57−1.69 (m, 1 H), 1.81−1.93 (m, 2 H), 1.94−2.04 (m, 2 H), 2.18−2.27 (m, 1 H), 2.30−2.40 (m, 1 H), 2.44−2.56 (m, 2 H), 2.78−2.90 (t, 2 H), 3.29−3.40 (m, 1 H), 3.55−3.67 (s, 3 H), 3.98−4.08 (m, 1 H), 4.38−4.46 (s, 2 H), 7.03−7.15 (m, 1 H), 7.82−7.93 (m, 1 H). HRMS (ESI) calcd for C$_{24}$H$_{38}$N$_6$O$_8$Na, [M + Na]$^+$: 561.2649. Found: 561.2643.

Methyl 14-((*tert*-Butoxycarbonyl)amino)-11-isobutyl-5,10,13-trioxo-4,9,12-triaza-1(2,5)-oxadiazolacyclohexadecaphane-8-carboxylate (9c). Yield (57%), mp 155−157 °C. ^{1}H NMR (400 MHz, DMSO-d_6) δ 0.80−0.93 (m, 6 H), 1.33−1.45 (s, 9 H), 1.84−1.97 (m, 2 H), 1.99−2.04 (m, 1 H), 2.78 (br s, 1 H), 2.79 (d, J = 5.08 Hz, 1 H), 2.85−2.97 (m, 2 H), 3.29−3.41 (m, 8 H), 3.56−3.68 (m, 3 H), 3.56−3.68 (m, 3 H), 4.37−4.45 (m, 1 H), 6.98−7.02 (dd, 1H), 7.30−7.35 (dd, 1H), 7.89−8.00 (dd, 1 H), 8.21 (dd, J = 11.55, 8.42 Hz, 1 H). HRMS (ESI) calcd for C$_{25}$H$_{40}$N$_6$O$_8$Na, [M + Na]$^+$: 575.2805. Found: 575.2824.

Methyl (8S,11S,14S)-14-((*tert*-Butoxycarbonyl)amino)-11-(cyclohexylmethyl)-5,10,13-trioxo-4,9,12-triaza-1(2,5)-oxadiazolacyclohexadecaphane-8-carboxylate (9d). Yield (70%), mp 197−200 °C. ^{1}H NMR (400 MHz, DMSO-d_6) δ 0.80−0.91 (m, 2 H), 1.07−1.20 (m, 3 H), 1.33−1.41 (m, 6 H), 1.38 (s, 9 H), 1.42−1.46 (m, 2 H), 1.58−1.67 (m, 4 H), 1.89−2.01 (m, 1 H), 2.47−2.56 (m, 2 H), 2.78−2.84 (m, 1 H), 2.86−2.93 (t, 2 H), 3.30−3.43 (t, 2 H), 3.55−3.67 (s, 3 H), 4.03 (d, J = 7.13 Hz, 1 H), 4.43−4.50 (t, 2 H), 7.89−8.00 (m, 1 H), 7.15 (dd, 1H), 7.3 (dd, 1H), 8.21 (dd, J = 11.55, 8.42 Hz, 1 H). HRMS (ESI) calcd for C$_{28}$H$_{44}$N$_6$O$_8$Na, [M + Na]$^+$: 615.3118. Found: 615.3112.

Methyl (9S,12S,15S)-15-((*tert*-Butoxycarbonyl)amino)-12-isobutyl-6,11,14-trioxo-5,10,13-triaza-1(2,5)-oxadiazolacycloheptadecaphane-9-carboxylate(9e). Yield (72%), mp 218−220 °C. ^{1}H NMR (400 MHz, DMSO-d_6) δ 0.81−0.93 (m, 6 H), 1.35 (s, 9 H), 1.62 (d, J = 6.79 Hz, 1 H), 1.80−1.89 (m, 4 H), 2.49 (br s, 1 H), 2.50 (dt, J = 3.75, 1.86 Hz, 4 H), 2.66−2.72 (m, 1 H), 2.73−2.79 (m, 2 H), 3.32 (s, 2 H), 3.32−3.35 (m, 4 H), 3.62 (s, 3 H), 4.37 (br s, 1 H), 4.37−4.44 (m, 1 H), 8.16−8.22 (m, 1 H),

8.39−8.46 (m, 1 H), 9.95 (s, 1 H). HRMS (ESI) calcd for C$_{26}$H$_{42}$N$_6$O$_8$, [M + Na]$^+$: 589.2962. Found: 589.2962.

Methyl (9S,12S,15S)-15-((*tert*-Butoxycarbonyl)amino)-12-(cyclohexylmethyl)-6,11,14-trioxo-5,10,13-triaza-1(2,5)-oxadiazolacycloheptadecaphane-9-carboxylate (9f). Yield (65%), mp 177−180 °C. ^{1}H NMR (400 MHz, DMSO-d_6) δ 0.79−0.91 (m, 2 H), 1.08−1.20 (m, 6 H), 1.40−1.43 (s, 9 H), 1.56−1.69 (m, 3 H), 1.75−1.88 (m, 4 H), 1.97−2.02 (m, 2 H), 2.09−2.21 (m, 1 H), 2.47−2.53 (m, 2 H), 2.68−2.78 (m, 3 H), 2.85−2.96 (m, 2 H), 3.17 (d, J = 4.83 Hz, 1 H), 3.33 (t, 2 H), 3.63−3.68 (s, 3 H), 3.97−4.06 (m, 2 H), 4.33−4.42 (m, 1 H), 6.88−7.00 (m, 1 H), 7.88−8.00 (m, 1 H), 8.37−8.45 (m, 1 H). HRMS (ESI) calcd for C$_{29}$H$_{46}$N$_6$O$_8$Na, [M + Na]$^+$: 629.3275. Found: 629.3267.

Methyl (4S,7S,10S)-4-((*tert*-Butoxycarbonyl)amino)-7-(cyclohexylmethyl)-5,8,13-trioxo-6,9,14-triaza-1(2,5)-oxadiazolacyclooctadecaphane-10-carboxylate (9g). Yield (51%), mp 98−101 °C. ^{1}H NMR (400 MHz, DMSO-d_6) δ 0.83−0.95 (m, 2 H), 1.09−1.21 (m, 3 H), 1.32−1.43 (m, 5 H), 1.36 (s, 9 H) 1.56−1.69 (m, 4 H), 1.75−1.88 (m, 4 H), 1.96−2.07 (m, 2 H), 2.09−2.23 (m, 2 H), 2.40−2.47 (m, 1 H), 2.49−2.53 (m, 1 H), 2.66−2.79 (m, 3 H), 2.84−2.93 (m, 1 H), 3.56−3.68 (s, 3 H), 3.95−4.06 (m, 2 H), 4.36−4.44 (m, 2 H), 6.66−6.75 (dd, J = 8.4 Hz, 1 H), 8.14−8.24 (dd, J = 8.2 Hz, 1 H), 8.38−8.45 (dd, J = 8.2 Hz, 1 H), 9.93−9.98 (m, 1 H). HRMS (ESI) calcd for C$_{30}$H$_{48}$N$_6$O$_8$Na, [M + Na]$^+$: 643.3431. Found: 643.3412.

Methyl (4S,7S,10S)-4-((*tert*-Butoxycarbonyl)amino)-7-(cyclohexylmethyl)-5,8,13-trioxo-6,9,14-triaza-1(2,5)-oxadiazolacyclooctadecaphane-10-carboxylate (9h). Yield (51%), mp 181−183 °C. ^{1}H NMR (400 MHz, CDCl$_3$) δ 0.77−0.90 (m, 2 H), 0.90−1.01 (m, 2 H), 1.12−1.20 (m, 4 H), 1.24−1.35 (m, 4 H), 1.37−1.46 (m, 6 H), 1.43 (s, 9 H), 1.50−1.58 (m, 2 H), 1.60−1.71 (m, 4 H), 1.72−1.80 (m, 3 H), 2.23−2.32 (m, 2 H), 2.88 (ddd, J = 10.79, 7.62, 4.64 Hz, 2 H), 2.98−3.10 (m, 2 H), 3.64−3.76 (s, 3 H), 4.51−4.61 (m, 1 H), 6.83−6.95 (m, 1 H), 7.39−7.50 (d, 1 H), 7.6−7.7 (d, 1 H), 7.8−7.9(d, 1 H). HRMS (ESI) calcd for C$_{31}$H$_{50}$N$_6$O$_8$Na, [M + Na]$^+$: 657.3588. Found: 657.3590.

Synthesis of Alcohols 10a−h. General Procedure. To a solution of ester **9** (3.25 mmol) in anhydrous THF (25 mL) was added dropwise lithium borohydride (2 M in THF, 4.9 mL, 9.75 mmol) followed by absolute ethyl alcohol (15 mL), and the reaction mixture was stirred at room temperature overnight. The reaction mixture was then acidified by adding 1.5 M potassium bisulfate until the pH of the solution was ~3. Removal of the solvent left a residue which was taken up in ethyl acetate (150 mL). The organic layer was washed with brine (25 mL), dried over anhydrous sodium sulfate, filtered, and concentrated to yield compounds **10a−h**.

tert-Butyl ((7S,10S,13S)-7-(Hydroxymethyl)-10-isobutyl-4,9,12-trioxo-3,8,11-triaza-1(2,5)-oxadiazolacyclotetradecaphane-13-yl)carbamate (10a). 170d °C, yield (82%). ^{1}H NMR (400 MHz, DMSO-d_6) δ 0.79−0.91 (m, 6 H), 1.15−1.20 (m, 1 H), 1.33−1.45 (s, 9 H), 1.53−1.65 (m, 2 H), 1.73−1.85 (m, 1 H), 1.86−1.96 (m, 1 H), 1.96−2.03 (m, 1 H), 2.15−2.27 (m, 1 H), 2.38 (br s, 1 H), 2.51 (dquin, J = 3.48, 1.74, 1.74, 1.74, 1.74 Hz, 1 H), 2.85−2.97 (m, 1 H), 3.19−3.26 (m, 1 H), 3.28−3.40 (m, 1 H), 3.62−3.73 (m, 1 H), 3.99−4.08 (m, 1 H), 4.27 (br s, 2 H), 7.31−7.38 (m, 1 H), 7.39−7.45 (m, 1 H), 7.51−7.62 (m, 1 H), 7.66−7.76 (m, 1 H), 7.90−8.02 (m, 1 H). HRMS (ESI) calcd for C$_{22}$H$_{37}$N$_6$O$_7$, [M + H]$^+$: 497.2724. Found: 497.2710.

tert-Butyl ((7S,10S,13S)-7-(Hydroxymethyl)-10-isobutyl-4,9,12-trioxo-3,8,11-triaza-1(2,5)-oxadiazolacyclopentadecaphane-13-yl)carbamate (10b). Yield (80%), mp 183−186 °C. ^{1}H NMR (400 MHz, DMSO-d_6) δ 0.78−0.90 (m, 6 H), 1.15−1.23 (m, 1 H), 1.38 (s, 9 H), 1.57−1.63 (m, 1 H), 1.70−1.81 (m, 1 H), 1.87−1.95 (m, 1 H), 2.48−2.56 (m, 3 H), 2.77−2.86 (m, 1 H), 2.88−2.98 (m, 1 H), 3.20−3.26 (m, 1 H), 3.29−3.42 (m, 2 H), 3.59−3.66 (m, 1 H), 3.66−3.75 (m, 1 H), 4.27 (br s, 2 H), 4.40−4.50 (m, 3 H), 6.99−7.03 (d, 1 H), 7.22−7.29 (d, 1 H), 7.62−7.70 (d, 1 H), 7.90−8.00 (d, 1 H). HRMS (ESI) calcd for C$_{23}$H$_{38}$N$_6$O$_7$Na, [M + Na]$^+$: 533.2700. Found: 533.2721.

tert-Butyl ((8S,11S,14S)-8-(Hydroxymethyl)-11-isobutyl-5,10,13-trioxo-4,9,12-triaza-1(2,5)-oxadiazolacyclohexa-

decaphane-14-yl)carbamate (10c).** Yield (85%), mp 181−184 °C. ¹H NMR (400 MHz, DMSO-d_6) δ 0.78−0.90 (m, 6 H), 1.15−1.23 (m, 1 H), 1.38 (br s, 9 H), 1.57−1.63 (m, 1 H), 1.70−1.81 (m, 1 H), 1.87−1.95 (m, 1 H), 1.97−2.09 (m, 1 H), 1.97−2.09 (m, 1 H), 2.48−2.56 (m, 3 H), 2.77−2.86 (m, 1 H), 2.88−2.98 (m, 2 H), 3.20−3.26 (m, 1 H), 3.29−3.42 (m, 4 H), 3.59−3.66 (m, 1 H), 3.66−3.75 (m, 1 H), 4.27 (br s, 2 H), 6.94−6.96 (d, 1 H), 7.09−7.13 (d, 1 H), 7.63−7.72 (d, 1 H), 7.90−8.02 (d, 1 H). HRMS (ESI) calcd for C₂₄H₄₀N₆O₇Na, [M + Na]⁺: 547.2856. Found: 547.2870.

tert-Butyl ((8S,11S,14S)-11-(Cyclohexylmethyl)-8-(hydroxymethyl)-5,10,13-trioxo-4,9,12-triaza-1(2,5)-oxadiazolacyclohexadecaphane-14-yl)carbamate (10d). Yield (88%), mp 188−191 °C. ¹H NMR (400 MHz, DMSO-d_6) δ 0.78−0.91 (m, 4 H), 1.07−1.18 (m, 6 H), 1.43−1.46 (s, 9 H), 1.56−1.67 (m, 1 H), 1.72−1.84 (m, 3 H), 1.97−2.09 (m, 2 H), 2.22−2.30 (m, 2 H), 2.44−2.50 (m, 2 H), 2.85−2.97 (m, 2 H), 3.55−3.67 (m, 5 H), 3.92−4.02 (m, 2 H), 4.25−4.37 (m, 2 H), 6.53 (br s, 1 H), 7.04−7.16 (m, 1 H), 7.67−7.80 (m, 1 H), 7.86−7.97 (m, 1 H). HRMS (ESI) calcd for C₂₇H₄₅N₆O₇, [M + H]⁺: 565.3350. Found: 565.3361.

tert-Butyl ((9S,12S,15S)-9-(Hydroxymethyl)-12-isobutyl-6,11,14-trioxo-5,10,13-triaza-1(2,5)-oxadiazolacycloheptadecaphane-15-yl)carbamate (10e). Yield (85%), mp 168−172 °C. ¹H NMR (400 MHz, DMSO-d_6) δ 0.85−0.97 (m, 6 H), 1.09−1.15 (m, 2 H), 1.16−1.23 (m, 2 H), 1.29 (br s, 1 H), 1.38−1.47 (s, 9 H), 1.58 (br s, 1 H), 1.58−1.68 (m, 2 H), 2.48−2.60 (m, 4 H), 2.67−2.76 (m, 1 H), 2.81−2.93 (m, 4 H), 3.48−3.61 (m, 3 H), 4.30−4.50 (m, 3 H), 7.36 (br s, 1 H), 7.37−7.45 (m, 2 H), 7.60−7.64 (d, 1 H). HRMS (ESI) calcd for C₂₅H₄₃N₆O₇, [M + H]⁺: 539.3193. Found: 539.0371.

tert-Butyl ((9S,12S,15S)-12-(Cyclohexylmethyl)-9-(hydroxymethyl)-6,11,14-trioxo-5,10,13-triaza-1(2,5)-oxadiazolacycloheptadecaphane-15-yl)carbamate (10f). Yield (90%), mp 191−194 °C. ¹H NMR (400 MHz, DMSO-d_6) δ 0.80−0.92 (m, 3 H), 1.08−1.20 (m, 4 H), 1.23−1.30 (m, 2 H), 1.35−1.47 (s, 9 H), 1.57−1.69 (m, 4 H), 1.81−1.85 (m, 1 H), 1.87−1.96 (m, 2 H), 1.96−2.07 (m, 2 H), 2.15 (br s, 2 H), 2.48−2.60 (m, 4 H), 2.67−2.76 (m, 1 H), 2.89−2.96 (m, 1 H), 3.54−3.62 (m, 3 H), 3.64−3.67 (m, 1 H), 4.18−4.30 (br s, 2 H), 7.31−7.33 (d, 1 H), 7.66−7.68 (d, 1 H), 7.81−7.84 (d, 1 H), 7.94−7.97 (d, 1 H). HRMS (ESI) calcd for C₂₈H₄₆N₆O₇Na, [M + Na]⁺: 601.3326. Found: 601.0944.

tert-Butyl ((4S,7S,10S)-7-(Cyclohexylmethyl)-10-(hydroxymethyl)-5,8,13-trioxo-6,9,14-triaza-1(2,5)-oxadiazolacyclooctadecaphane-4-yl)carbamate (10g). Yield (92%), mp 139−141 °C. ¹H NMR (400 MHz, DMSO-d_6) δ 0.79−0.92 (m, 2 H), 1.05−1.14 (m, 5 H), 1.23−1.30 (m, 2 H), 1.43−1.46 (s, 9 H), 1.56−1.67 (m, 4 H), 1.82−1.87 (m, 2 H), 1.89−1.97 (m, 3 H), 2.15−2.26 (m, 1 H), 2.48−2.59 (m, 2 H), 2.67−2.73 (m, 1 H), 2.74−2.86 (m, 2 H), 2.88−2.95 (m, 1 H), 3.22−3.27 (m, 1 H), 3.30−3.39 (m, 2 H), 3.41−3.47 (m, 1 H), 3.60−3.71 (m, 1 H), 3.92−4.02 (m, 2 H), 4.25−4.37 (m, 2 H), 6.53 (br s, 1 H), 7.04−7.16 (m, 1 H), 7.67−7.80 (m, 1 H), 7.86−7.97 (m, 1 H). HRMS (ESI) calcd for C₂₉H₄₉N₆O₇, [M + H]⁺: 593.3663. Found: 593.3660.

tert-Butyl ((4S,7S,10S)-7-(Cyclohexylmethyl)-10-(hydroxymethyl)-5,8,13-trioxo-6,9,14-triaza-1(2,5)-oxadiazolacyclononadecaphane-4-yl)carbamate (10h). Yield (90%), mp 142−145 °C. ¹H NMR (400 MHz, CDCl₃) δ 0.84−0.96 (m, 2 H), 1.12−1.21 (m, 5 H), 1.24−1.28 (m, 2 H), 1.37−1.48 (s, 9 H), 1.60−1.71 (m, 7 H), 1.84 (d, J = 2.64 Hz, 1 H), 1.84−1.96 (m, 2 H), 1.96−2.07 (m, 2 H), 2.09 (s, 1 H), 2.16−2.28 (m, 2 H), 2.28−2.40 (m, 2 H), 2.80−2.92 (m, 2 H), 2.96 (br s, 2 H), 3.55−3.67 (m, 1 H), 3.75 (br s, 1 H), 4.12 (q, J = 7.11 Hz, 1 H), 4.40−4.50 (m, 2 H), 7.26−7.35 (m, 2 H), 7.40−7.53 (m, 2 H), 7.73−7.81 (m, 1 H), 7.81−7.93 (m, 1 H). HRMS (ESI) calcd for C₃₀H₅₀N₆O₇Na, [M + Na]⁺: 629.3639. Found: 629.3638.

Synthesis of Compounds 13a−d. General Procedure. To a solution of compound **4** (12.0 g, 26.75 mmol) in dry DMF (120 mL) were added EDCI (6.7 g, 34.78 mmol, 1.3 equiv), HOBt (5.29 g, 34.78 mmol, 1.3 equiv), and the mixture was stirred for 30 min at room temperature. In a separate flask, a solution of (L)-cyclohexyl alanine methyl ester hydrochloride **12** (5.93 g, 26.75 mmol) in dry DMF (100 mL) cooled to 0−5 °C was treated with diisopropylethylamine (13.83 g, 107 mmol, 4.0 equiv), stirred for 30 min, and then added to the

reaction mixture above. The solution was stirred for 16 h while monitoring the reaction by TLC. The solvent was removed, and the residue was partitioned between ethyl acetate (300 mL) and 5% aqueous HCl (2 × 120 mL). The ethyl acetate layer was further washed with saturated NaHCO₃ (2 × 120 mL), followed by saturated NaCl (120 mL). The organic layer was dried over anhydrous Na₂SO₄, filtered, and concentrated. The crude product was purified by flash chromatography to yield compounds **13a−d**.

Methyl (S)-2-((S)-4-(5-(2-(((Benzyloxy)carbonyl)amino)ethyl)-1,3,4-oxadiazol-2-yl)-2-((tert-butoxycarbonyl)amino)-butanamido)-3-cyclohexylpropanoate (13a). Oil, yield (80%). ¹H NMR (400 MHz, CDCl3) δ 0.85−0.98 (m, 2 H), 1.13−1.22 (m, 3 H), 1.23−1.26 (m, 1 H), 1.34−1.46 (m, 1H), 1.40 (s, 9 H), 1.60−1.72 (m, 6 H), 2.01−2.13 (m, 2 H), 2.18−2.31 (m, 1 H), 2.96−3.08 (m, 4 H), 3.62−3.74 (m, 2 H), 3.70 (s, 3 H), 4.15−4.26 (m, 1 H), 4.54−4.66 (m, 1 H), 5.05−5.17 (s, 2 H), 5.40−5.49 (m, 1 H), 5.71−5.84 (m, 1 H), 7.27−7.40 (m, 5 H). HRMS (ESI) calcd for C₃₁H₄₆N₅O₈, [M + H]⁺: 616.3346. Found: 616.3404.

Methyl (S)-2-((S)-4-(5-(3-(((Benzyloxy)carbonyl)amino)-propyl)-1,3,4-oxadiazol-2-yl)-2-((tert-butoxycarbonyl)amino)-butanamido)-3-cyclohexylpropanoate (13b). Oil, yield (81%). ¹H NMR (400 MHz, CDCl3) δ 0.84−0.96 (m, 3 H), 1.14−1.26 (m, 4 H), 1.34−1.46 (m, 3 H), 1.42 (s, 9 H), 1.59−1.72 (m, 3 H), 1.95−2.07 (m, 4 H), 2.23−2.35 (m, 1 H), 2.88 (t, J = 7.40 Hz, 2 H), 2.93−3.05 (m, 2 H), 3.23−3.36 (m, 2 H), 3.72−3.77 (s, 3 H), 4.17−4.29 (m, 1 H), 4.55−4.67 (m, 1 H), 5.09 (s, 2 H), 5.42 (d, J = 7.32 Hz, 1 H), 7.27−7.39 (m, 5 H). HRMS (ESI) calcd for C₃₂H₄₈N₅O₈, [M + H]⁺: 630.3503. Found: 630.3500.

Methyl (S)-2-((S)-4-(5-(4-(((Benzyloxy)carbonyl)amino)-butyl)-1,3,4-oxadiazol-2-yl)-2-((tert-butoxycarbonyl)amino)-butanamido)-3-cyclohexylpropanoate (13c). Oil, yield (81%). ¹H NMR (400 MHz, CDCl₃) δ 0.87−0.97 (m, 2 H), 1.14−1.26 (m, 2 H), 1.33−1.44 (s, 9 H), 1.58−1.63 (m, 2 H), 1.65−1.72 (m, 4 H), 1.77−1.85 (m, 2 H), 2.01−2.12 (m, 2 H), 2.22−2.34 (m, 2 H), 2.78−2.90 (m, 2 H), 2.98−3.08 (m, 1 H), 3.18−3.27 (m, 2 H), 3.68−3.75 (m, 2 H), 3.71 (s, 3 H), 4.19−4.27 (m, 1 H), 4.55−4.62 (m, 1 H), 5.01 (br s, 1 H), 5.09 (s, 2 H), 5.41 (d, J = 7.66 Hz, 1 H), 7.13−7.24 (m, 1 H), 7.26−7.39 (m, 5 H). HRMS (ESI) calcd for C₃₃H₅₀N₅O₈, [M + H]⁺: 644.3659. Found: 644.3652.

Methyl (S)-2-((R)-4-(5-(5-(((Benzyloxy)carbonyl)amino)-pentyl)-1,3,4-oxadiazol-2-yl)-2-((tert-butoxycarbonyl)amino)-butanamido)-3-cyclohexylpropanoate (13d). Oil, yield (79%). ¹H NMR (400 MHz, CDCl₃) δ 0.86−0.99 (m, 2 H), 1.14−1.20 (m, 2 H), 1.21−1.28 (m, 2 H), 1.35−1.47 (s, 9 H), 1.52−1.59 (m, 2 H), 1.61−1.72 (m, 6 H), 1.74−1.82 (m, 2 H), 1.96−2.07 (m, 2 H), 2.22−2.35 (m, 1 H), 2.77−2.89 (m, 2 H), 2.93−3.05 (m, 2 H), 3.12−3.25 (m, 2 H), 3.67−3.78 (s, 3 H), 4.24−4.30 (br s, 1 H), 4.55−4.67 (m, 1 H), 5.04−5.16 (s, 2 H), 5.35−5.55 (br s, 1H), 6.98−7.0 (br s, 1 H), 7.27−7.39 (m, 5 H). HRMS (ESI) calcd for C₃₄H₅₂N₅O₈, [M + H]⁺: 658.3816. Found: 658.3879.

Synthesis of Compounds 14a−d. General Procedure. A solution of ester **13** (25 mmol) in THF (40 mL) was treated with 1 M LiOH in aqueous ethanol (50 mL). The reaction mixture was stirred for 3 h at room temperature, and the disappearance of the ester was monitored by TLC. Most of the solvent was evaporated off, and the residue was diluted with water (25 mL). The solution was acidified to pH ≈ 3 using 5% hydrochloride acid (25 mL), and the aqueous layer was extracted with ethyl acetate (3 × 100 mL). The combined organic layers were dried over anhydrous sodium sulfate, filtered, and concentrated to yield compounds **14a−d**.

(S)-2-((S)-4-(5-(2-(((Benzyloxy)carbonyl)amino)ethyl)-1,3,4-oxadiazol-2-yl)-2-((tert-butoxycarbonyl)amino)butanamido)-3-cyclohexylpropanoic Acid (14a). Yield (95%), mp 59−62 °C. ¹H NMR (400 MHz, CDCl3) δ 0.85−0.98 (m, 2 H), 1.13−1.22 (m, 3 H), 1.23−1.26 (m, 1 H), 1.34−1.46 (m, 1H), 1.40 (s, 9 H), 1.60−1.72 (m, 6 H), 2.01−2.13 (m, 2 H), 2.18−2.31 (m, 1 H), 2.96−3.08 (m, 4 H), 3.62−3.74 (m, 2 H), 4.15−4.26 (m, 1 H), 4.54−4.66 (m, 1 H), 5.05−5.17 (s, 2 H), 5.40−5.49 (m, 1 H), 5.71−5.84 (m, 1 H), 7.27−7.40 (m, 5 H). HRMS (ESI) calcd for C₃₀H₄₄N₅O₈, [M + H]⁺: 602.3190. Found: 602.3214.

(S)-2-((S)-4-(5-(3-(((Benzyloxy)carbonyl)amino)propyl)-1,3,4-oxadiazol-2-yl)-2-((*tert*-butoxycarbonyl)amino)butanamido)-3-cyclohexylpropanoic Acid (14b). Oil, yield (95%). ^{1}H NMR (400 MHz, CDCl3) δ 0.84−0.96 (m, 3 H), 1.14−1.26 (m, 4 H), 1.34−1.46 (m, 3 H), 1.42 (s, 9 H), 1.59−1.72 (m, 3 H), 1.95−2.07 (m, 4 H), 2.23−2.35 (m, 1 H), 2.88 (t, J = 7.40 Hz, 2 H), 2.93−3.05 (m, 2 H), 3.23−3.36 (m, 2 H), 4.17−4.29 (m, 1 H), 4.55−4.67 (m, 1 H), 5.09 (s, 2 H), 5.42 (d, J = 7.32 Hz, 1 H), 7.27−7.39 (m, 5 H). HRMS (ESI) calcd for $C_{31}H_{46}N_5O_8$, $[M + H]^+$: 616.3346. Found: 616.3362.

(S)-2-((R)-4-(5-(4-(((Benzyloxy)carbonyl)amino)butyl)-1,3,4-oxadiazol-2-yl)-2-((*tert*-butoxycarbonyl)amino)butanamido)-3-cyclohexylpropanoic Acid (14c). Oil, yield (98%). ^{1}H NMR (400 MHz, CDCl$_3$) δ 0.87−0.98 (m, 2 H), 1.14−1.26 (m, 2 H), 1.39−1.50 (s, 9 H), 1.56−1.62 (m, 2 H), 1.64−1.71 (m, 4 H), 1.74−1.82 (m, 4 H), 2.02−2.15 (m, 2 H), 2.23−2.34 (m, 1 H), 2.81−2.91 (m, 2 H), 2.92−3.00 (m, 1 H), 3.14−3.26 (m, 2 H), 4.30−4.42 (m, 1 H), 4.57−4.69 (m, 1 H), 5.06−5.18 (s, 2 H), 5.18−5.30 (m, 1 H), 5.43−5.53 (m, 1 H), 5.53−5.65 (m, 1 H), 6.66−6.78 (m, 1 H), 7.26−7.39 (m, 5 H). HRMS (ESI) calcd for $C_{32}H_{48}N_5O_8$, $[M + H]^+$: 630.3503. Found: 630.3570.

(S)-2-((R)-4-(5-(5-(((Benzyloxy)carbonyl)amino)pentyl)-1,3,4-oxadiazol-2-yl)-2-((*tert*-butoxycarbonyl)amino)butanamido)-3-cyclohexylpropanoic Acid (14d). Oil, yield (98%). ^{1}H NMR (400 MHz, CDCl$_3$) δ 0.86−0.99 (m, 2 H), 1.14−1.20 (m, 2 H), 1.21−1.28 (m, 2 H), 1.35−1.47 (s, 9 H), 1.52−1.59 (m, 2 H), 1.61−1.72 (m, 6 H), 1.74−1.82 (m, 2 H), 1.96−2.07 (m, 2 H), 2.22−2.35 (m, 1 H), 2.77−2.89 (m, 2 H), 2.93−3.05 (m, 2 H), 3.12−3.25 (m, 2 H), 4.24−4.30 (br s 1 H), 4.55−4.67 (m, 1 H), 5.04−5.16 (s, 2 H), 5.35−5.55 (br s, 1H), 6.98−7.0 (br s, 1 H), 7.27−7.39 (m, 5 H). HRMS (ESI) calcd for $C_{33}H_{50}N_5O_8$, $[M + H]^+$: 644.3659. Found: 644.3742.

Synthesis of Compounds 7d and 7f−h. General Procedure. To a solution of compound **14** (15.0 g, 24.92 mmol) in dry DMF (150 mL) were added EDCI (6.2 g, 32.39 mmol, 1.3 equiv), HOBt (4.96 g, 32.39 mmol, 1.3 equiv), and the reaction mixture was stirred for 30 min at room temperature. In a separate flask, a solution of (L)-Glu(OBzl) methyl ester hydrochloride **5** (7.17 g, 24.92 mmol) in dry DMF (80 mL) cooled to 0−5 °C was treated with diisopropylethylamine (DIEA) (12.88 g, 99.68 mmol, 4.0 equiv), stirred for 30 min, and then added to the reaction mixture above. The reaction mixture was stirred for 16 h while monitoring the reaction by TLC. The solvent was removed, and the residue was partitioned between ethyl acetate (400 mL) and 5% aqueous HCl (2 × 120 mL). The ethyl acetate layer was further washed with saturated aqueous NaHCO$_3$ (2 × 120 mL), followed by saturated NaCl (120 mL). The organic layer was dried over anhydrous Na$_2$SO$_4$, filtered, and concentrated. The crude was purified by flash chromatography to yield compounds **7d** and **7f−h**.

5-Benzyl 1-Methyl ((S)-2-((S)-4-(5-(2-(((Benzyloxy)carbonyl)amino)ethyl)-1,3,4-oxadiazol-2-yl)-2-((*tert*-butoxycarbonyl)amino)butanamido)-3-cyclohexylpropanoyl)-L-glutamate (7d). Yield (75%), mp 54−57 °C ^{1}H NMR (400 MHz, CDCl$_3$) δ 0.83−0.95 (m, 2 H), 1.12−1.20 (m, 2 H), 1.24−1.28 (m, 1 H), 1.37−1.48 (s, 9 H), 1.61−1.74 (m, 6 H), 1.96−2.08 (t, 2 H), 2.15−2.27 (m, 2 H), 2.19 (s, 2 H), 2.36−2.49 (m, 2 H), 2.87−2.96 (m, 2 H), 2.97−3.03 (m, 1 H), 3.60−3.72 (m, 2 H), 3.60−3.72 (s, 3 H), 4.11−4.20 (m, 1 H), 4.50−4.63 (m, 2 H), 5.06−5.18 (s,s, 4 H), 7.09−7.18 (m, 1 H), 7.29−7.39 (m, 10 H), 8.2−8.3 (dd, 2 H). HRMS (ESI) calcd for $C_{43}H_{59}N_6O_{11}$, $[M + H]^+$: 835.4242. Found: 835.4238.

(S)-5-Benzyl 1-Methyl (2-(4-(5-(3-(((Benzyloxy)carbonyl)amino)propyl)-1,3,4-oxadiazol-2-yl)-2-((*tert*-butoxycarbonyl)amino)butanamido)-3-yclohexylpropanoyl)glutamate (7f). Oil, yield (70%). 1H NMR (400 MHz, CDCl$_3$) δ 0.82−0.94 (m, 2 H), 1.08−1.20 (m, 3 H), 1.22−1.26 (m, 1 H), 1.28−1.33 (m, 1 H), 1.35−1.44 (m, 1 H), 1.39 (s, 9 H), 1.58−1.70 (m, 5 H), 1.94−2.06 (m, 4 H), 2.14−2.26 (m, 2 H), 2.36−2.48 (m, 2 H), 2.81−2.93 (m, 3 H), 3.19−3.31 (m, 1 H), 3.61−3.72 (m, 3 H), 4.07−4.18 (m, 1 H), 4.40−4.49 (m, 2 H), 4.50−4.60 (m, 2 H), 5.02−5.14 (m, 4 H), 7.02−7.14 (m, 1 H), 7.25−7.37 (m, 10 H). HRMS (ESI) calcd for $C_{44}H_{61}N_6O_{11}$, $[M + H]^+$: 849.4398. Found: 849.4393.

5-Benzyl 1-Methyl ((S)-2-((S)-4-(5-(4-(((Benzyloxy)carbonyl)amino)butyl)-1,3,4-oxadiazol-2-yl)-2-((*tert*-butoxycarbonyl)amino)butanamido)-3-cyclohexylpropanoyl)-L-glutamate (7g). Yield (75%), mp 75−77 °C. ^{1}H NMR (400 MHz, CDCl3) δ 0.85−0.97 (m, 2 H), 1.10−1.22 (m, 2 H), 1.38−1.48 (s, 9 H), 1.58−1.71 (m, 5 H), 1.78−1.83 (m, 4 H), 1.96−2.09 (m, 2 H), 2.16−2.28 (m, 2 H), 2.37−2.48 (m, 2 H), 2.79−2.86 (m, 2 H), 2.87−2.97 (m, 2 H), 3.15−3.27 (m, 2 H), 3.66−3.77 (s, 3 H), 4.41−4.51 (m, 1 H), 4.53−4.62 (m, 1 H), 5.05−5.16 (m, 4 H), 7.03−7.16 (m, 1 H), 7.26−7.39 (m, 10 H). HRMS (ESI) calcd for $C_{45}H_{63}N_6O_{11}$, $[M + H]^+$: 863.4555. Found: 863.4549.

5-Benzyl 1-Methyl ((S)-2-((S)-4-(5-(5-(((Benzyloxy)carbonyl)amino)pentyl)-1,3,4-oxadiazol-2-yl)-2-((*tert*-butoxycarbonyl)amino)butanamido)-3-cyclohexylpropanoyl)-L-glutamate (7h). Yield (80%), mp 59−62 °C. ^{1}H NMR (400 MHz, CDCl$_3$) δ 0.85−0.97 (m, 2 H), 1.12−1.22 (m, 2 H), 1.24−1.28 (m, 2 H), 1.36−1.46 (m, 4 H), 1.42 (s, 9 H), 1.49−1.58 (m, 2 H), 1.63−1.72 (m, 4 H), 1.74−1.76 (m, 2 H), 1.96−2.08 (m, 2 H), 2.16−2.29 (m, 2 H), 2.37−2.49 (m, 2 H), 2.76−2.83 (m, 2 H), 2.86−2.98 (m, 2 H), 3.11−3.24 (m, 2 H), 3.66−3.76 (s, 3 H), 4.0−4.15 (br s, 1H), 4.54−4.64 (m, 2 H), 5.04−5.16 (m, 4 H), 7.02−7.15 (m, 1 H), 7.27−7.39 (m, 10 H). HRMS (ESI) calcd for $C_{46}H_{65}N_6O_{11}$, $[M + H]^+$: 877.4711. Found: 877.4706.

Synthesis of Aldehydes 15−22. General Procedure. Compound **10** (0.95 mmol) was dissolved in anhydrous dichloromethane (30 mL) under a nitrogen atmosphere and cooled to 0 °C. Dess−Martin periodinane reagent (1.21 g, 2.85 mmol, 3.0 equiv) was added to the reaction mixture with stirring. The ice bath was removed, and the reaction mixture was stirred at room temperature for 3 h (monitoring by TLC indicated complete disappearance of the starting material). A solution of 40 mM sodium thiosulfate in saturated aqueous NaHCO$_3$ (50 mL) was added, and the solution was stirred for another 15 min. The aqueous layer was removed, and the organic layer was washed with sodium bicarbonate (25 mL), water (2 × 25 mL), and brine (25 mL). The organic layer was dried over anhydrous sodium sulfate, filtered, and concentrated. The yellow residue was purified by flash chromatography (silica gel/methylene chloride/ethyl acetate/methanol) to yield aldehydes **15−22**.

***tert*-Butyl ((7S,10S,13S)-7-Formyl-10-isobutyl-4,9,12-trioxo-3,8,11-triaza-1(2,5)-oxadiazolacyclotetradecaphane-13-yl)carbamate (15).** Yield (43%), mp 91−94 °C. ^{1}H NMR (400 MHz, CDCl$_3$) δ 0.84−0.97 (m, 6 H), 1.17−1.30 (m, 1 H), 1.38−1.50 (s, 9 H), 1.63−1.71 (m, 2 H), 2.37−2.48 (m, 2 H), 2.54−2.63 (m, 2 H), 2.90−2.97 (m, 1 H), 3.12−3.19 (m, 1 H), 4.35−4.43 (m, 2 H), 4.50−4.61 (s, 2 H), 4.65−4.70 (m, 1 H), 6.94−7.01 (d, 1 H), 7.18−7.23 (d, 1 H), 7.79−7.91 (d, 1 H), 8.14−8.19 (d, 1 H), 9.55−9.60 (s, 1 H). HRMS (ESI) calcd for $C_{22}H_{35}N_6O_7$, $[M + H]^+$: 495.2567. Found: 495.2887.

***tert*-Butyl ((7S,10S,13S)-7-Formyl-10-isobutyl-4,9,12-trioxo-3,8,11-triaza-1(2,5)-oxadiazolacyclopentadecaphane-13-yl)carbamate (16).** Yield (40%), mp 99−102 °C. ^{1}H NMR (400 MHz, CDCl$_3$) δ 0.84−0.97 (m, 6 H), 1.17−1.30 (m, 1 H), 1.38−1.50 (s, 9 H), 1.63−1.71 (m, 3 H), 2.37−2.48 (m, 3 H), 2.54−2.63 (m, 2 H), 2.88−2.97 (m, 2 H), 4.35−4.43 (m, 3 H), 4.45−4.56 (s, 2 H), 6.94−7.01 (d, 1 H), 7.18−7.23 (d, 1 H), 7.79−7.91 (d, 1 H), 8.14−8.19 (d, 1 H), 9.55−9.60 (s, 1 H). HRMS (ESI) calcd for $C_{23}H_{36}N_6O_7Na$, $[M + Na]^+$: 531.2543. Found: 531.2520.

***tert*-Butyl ((8S,11S,14S)-8-Formyl-11-isobutyl-5,10,13-trioxo-4,9,12-triaza-1(2,5)-oxadiazolacyclohexadecaphane-14-yl)carbamate (17).** Yield (45%), mp 76−78 °C. ^{1}H NMR (400 MHz, CDCl3) δ 0.83−0.95 (d, 6 H), 1.11−1.23 (m, 1 H), 1.26 (br s, 2 H), 1.43−1.46 (s, 9 H), 1.56−1.69 (m, 3 H), 2.37−2.50 (m, 2 H), 2.89−3.00 (m, 3 H), 3.01−3.05 (m, 1 H), 3.42−3.54 (m, 1 H), 3.57−3.69 (m, 2 H), 4.47−4.52 (m, 3 H), 7.26−7.30 (m, 1 H), 7.09−7.13 (d, 1 H), 7.63−7.72 (d, 1 H), 7.90−8.02 (d, 1 H), 9.50−9.52 (s, 1 H). HRMS (ESI) calcd for $C_{24}H_{38}N_6O_6$, $[M + H]^+$: 523.28. Found: 523.3.

***tert*-Butyl ((8S,11S,14S)-11-(Cyclohexylmethyl)-8-formyl-5,10,13-trioxo-4,9,12-triaza-1(2,5)-oxadiazolacyclohexadecaphane-14-yl)carbamate (18).** Yield (50%), mp 106−108 °C. ^{1}H NMR (400 MHz, CDCl3) δ 0.84−0.96 (m, 4 H), 1.11−1.21 (m, 4 H), 1.44−1.48 (s, 9 H), 1.59−1.71 (m, 2 H), 2.00−2.13 (m, 2 H),

2.15−2.27 (m, 2 H), 2.38−2.49 (m, 2 H), 2.85−2.97 (m, 2 H), 3.55−3.67 (m, 5 H), 3.92−4.02 (m, 2 H), 4.37−4.46 (m, 3 H), 7.26−7.38 (m, 1 H), 7.67−7.80 (d, 1 H), 7.86−7.97 (d, 1 H), 8.20−8.23 (d, 1 H), 9.49−9.51 (s, 1 H). HRMS (ESI) calcd for $C_{27}H_{42}N_6O_6Na$, [M + Na]$^+$: 585.3013. Found: 585.3002.

tert-Butyl ((9S,12S,15S)-9-Formyl-12-isobutyl-6,11,14-trioxo-5,10,13-triaza-1(2,5)-oxadiazolacycloheptadecaphane-15-yl)-carbamate (19). Yield (45%), mp 86−88 °C. ^{1}H NMR (400 MHz, CDCl$_3$) δ 0.84−0.97 (m, 6 H), 1.17−1.30 (m, 1 H), 1.38−1.50 (s, 9 H), 1.63−1.71 (m, 3 H), 1.97−2.09 (m, 4 H), 2.37−2.48 (m, 2 H), 2.54−2.63 (m, 2 H), 2.88−2.97 (m, 1 H), 3.63−3.71 (m, 1 H), 3.73−3.85 (m, 2 H), 4.19−4.30 (m, 1 H), 4.35−4.43 (m, 1 H), 4.45−4.56 (m, 2 H), 6.97−7.06 (d, 1 H), 7.10−7.18 (d, 1 H), 7.99−8.05 (d, 1 H), 8.24−8.33 (d, 1 H), 9.52−9.60 (s, 1 H). HRMS (ESI) calcd for $C_{27}H_{38}N_6O_7Na$, [M + Na]$^+$: 545.2700. Found: 545.2613.

tert-Butyl ((9S,12S,15S)-12-(Cyclohexylmethyl)-9-formyl-6,11,14-trioxo-5,10,13-triaza-1(2,5)-oxadiazolacyclohepta-decaphane-15-yl)carbamate (20). Yield (45%), mp 96−99 °C. ^{1}H NMR (400 MHz, CDCl$_3$) δ 0.85−0.98 (m, 4 H), 1.10−1.22 (m, 6 H), 1.43−1.46 (s, 9 H), 1.60−1.72 (m, 3 H), 1.90−1.96 (m, 2 H), 1.98−2.08 (m, 4 H), 2.31−2.43 (m, 2 H), 2.86−2.98 (m, 4 H), 3.44−3.51 (m, 1 H), 3.85 (td, J = 5.97, 3.59 Hz, 2 H), 3.90−4.02 (m, 1 H), 4.27−4.39 (m, 2 H), 4.49 (br s, 1 H), 5.94−6.07 (d, 1 H), 6.87−6.98 (br s, 1 H), 7.87−7.92 (d, 1 H), 8.00−8.05 (d, 1 H), 9.48−9.59 (d, 1 H). HRMS (ESI) calcd for $C_{28}H_{45}N_6O_7$, [M + H]$^+$: 577.3350. Found: 577.3145.

tert-Butyl ((4S,7S,10S)-7-(Cyclohexylmethyl)-10-formyl-5,8,13-trioxo-6,9,14-triaza-1(2,5)-oxadiazolacyclooctade-decaphane-4-yl)carbamate (21). Yield (52%), mp 80−83 °C. ^{1}H NMR (400 MHz, CDCl$_3$) δ 0.85−0.98 (m, 4 H), 1.10−1.22 (m, 6 H), 1.43−1.46 (s, 9 H), 1.60−1.72 (m, 3 H), 1.90−1.96 (m, 2 H), 1.98−2.08 (m, 4 H), 2.31−2.43 (m, 2 H), 2.86−2.98 (m, 4 H), 3.44−3.51 (m, 1 H), 3.85 (td, J = 5.97, 3.59 Hz, 2 H), 3.90−4.02 (m, 1 H), 4.27−4.39 (m, 2 H), 4.49 (br s, 1 H), 7.02−7.10 (d, 1 H), 7.31−7.40 (br s, 1 H), 7.77−7.81 (d, 1 H), 8.01−8.05 (d, 1 H), 9.48−9.59 (d, 1 H). HRMS (ESI) calcd for $C_{29}H_{46}N_6O_7Na$, [M + Na]$^+$: 613.3326. Found: 613.3299.

tert-Butyl ((4S,7S,10S)-7-(Cyclohexylmethyl)-10-formyl-5,8,13-trioxo-6,9,14-triaza-1(2,5)-oxadiazolacyclonona-decaphane-4-yl)carbamate (22). Yield (50%), mp 106−109 °C. ^{1}H NMR (400 MHz, CDCl3) δ 0.87−0.99 (m, 4 H), 1.14−1.23 (m, 4 H), 1.34−1.37 (m, 1 H), 1.44−1.54 (s, 9 H), 1.63−1.75 (m, 8 H), 2.01−2.12 (m, 2 H), 2.12−2.24 (m, 4 H), 2.30 (br s, 2 H), 2.87−2.97 (m, 2 H), 3.43−3.55 (m, 4 H), 4.37−4.49 (m, 3 H), 6.74−6.84 (m, 1 H), 7.11−7.23 (m, 1 H), 7.46−7.54 (d, 1 H), 7.98−8.06 (m, 1 H), 9.50−9.55 (s, 1 H). HRMS (ESI) calcd for $C_{30}H_{48}N_6O_7Na$, [M + Na]$^+$: 627.3482. Found: 627.3465.

Enzyme Assays and Inhibition Studies. These studies were carried out as described previously.[26,28,41] The NV 3CLpro fluorescence resonance energy transfer (FRET) assay was performed using a fluorogenic substrate (Edans-DFHLQGP-Dabcyl) which is derived from the cleavage sites on NV polyproteins. Methods for FRET assay and determination of the IC$_{50}$ values of protease inhibitors against 3CLpro were described previously by our lab.[26,28,41]

Antiviral Assays. Each compound was evaluated for anti-3CLpro effects up to 100 μM. For the cell based assay, 1 day old HG23 cells (NV replicon harboring cells) were treated with various concentrations (1.0−100 μM) of each compound and incubated for 48 h. Then total RNA was extracted from cells for qRT-PCR for norovirus and β-actin. The EC$_{50}$ and EC$_{90}$ (the 50% and 90% inhibitory concentration in cell based assay, respectively) of each compound were calculated by the % reduction of RNA levels to Mock-treated cells after normalization with β-actin levels. Each compound was also tested against MNV-1. Confluent RAW267.4 was inoculated with MNV-1 at a MOI of 0.05, and at the same time, various concentrations (1.0−100 μM) of each compound were added to the medium. Virus infected cells were further incubated for 72 h until extensive cytopathic effects (CPE) progress. The EC$_{50}$ of each compound was determined by 50% inhibition of CPE progress (cell death) by each compound at 48 h using a CytoTox96 nonradioactive cytotoxicity assay kit (Promega, Madison, WI) following the manufacturer's instructions. Cell cytotoxicity for each compound in HG23 cells was also measured by the cytotoxicity assay kit with serial dilution up to 100 μM. The CC$_{50}$ (the 50% cytotoxic concentration) was determined for each compound. The IC$_{50}$, EC$_{50}$, or CC$_{50}$ values were determined by at least two independent experiments.

X-ray Crystallographic Studies. Crystallization and Data Collection. Purified norovirus 3CL protease (3CLpro) in 100 mM NaCl, 50 mM PBS, pH 7.2, 1 mM DTT at a concentration of 10 mg/mL was used for the preparation of the enzyme:22 complex. Stock solutions of 100 mM 21 and 22 were prepared in DMSO and the 3CLpro:inhibitor complex was prepared by mixing 7 μL of the inhibitors (3 mM) with 243 μL (0.49 mM) of 3CLpro and incubating on ice for 1 h. The buffer was exchanged to 100 mM NaCl, 20 mM Tris, pH 8.0, using a Zeba spin desalting column (MWCO = 7 kDa, Life Technologies), and the sample was concentrated to 10.0 mg/mL for crystallization screening. All crystallization experiments were conducted using a Compact Jr. (Rigaku Reagents) sitting drop vapor diffusion plates at 20 °C and equal volumes of protein and crystallization solution equilibrated against 75 μL of the latter. Crystals were obtained from the from the Index HT screen (Hampton Research). Prismatic crystals of NV 3CLpro:21 were obtained in 2 days from condition E9 (30% v/v pentaerythritol ethoxylate (15/4 EO/OH), 50 mM Bis-Tris, pH 6.5, 50 mM ammonium sulfate). Crystals of NV 3CLpro:22 displaying a needle morphology were obtained in 2−3 days condition H12 (30% (w/v) PEG 2000 MME, 150 mM potassium bromide). Samples were cryoprotected in a fresh drop crystallant for NV 3CLpro:21 and 80% crystallization solution/20% glycerol for NV 3CLpro:22, before storing in liquid nitrogen. X-ray diffraction data were collected at the Advanced Photon Source beamline 17-ID using a Dectris Pilatus 6M pixel array detector.

Structure Solution and Refinement. Intensities were integrated using XDS,[44,45] and the Laue class analysis and data scaling were performed with Aimless[46] which suggested that the highest probability Laue class was 2/m (C2) for NV 3CLpro:21 and mmm (P2$_1$2$_1$2$_1$) for NV 3CLpro:22. Structure solution was conducted by molecular replacement with Phaser[47] using a previously determined isomorphous structure of inhibitor bound norovirus 3CLpro (PDB code 3UR9) as the search model. Structure refinement and manual model building were conducted with Phenix[48] and Coot,[49] respectively. Disordered side chains were truncated to the point for which electron density could be observed. All atoms were refined with anisotropic atomic displacement parameters for NV 3CLpro:21. Structure validation was conducted with Molprobity,[50] and figures were prepared using the CCP4MG package.[51] Coordinates and structure factors were deposited to the wwPDB with the accession codes 5DGJ (NV 3CLpro:21) and 5DG6 (NV 3CLpro:22).

■ ASSOCIATED CONTENT

ⓢ Supporting Information

The Supporting Information is available free of charge on the ACS Publications website at DOI: 10.1021/acs.jmed-chem.5b01464.

Molecular formula strings (CSV)

Accession Codes

Coordinates and structure factors were deposited to the wwPDB with accession codes 5DGJ (NV 3CLpro:21) and 5DG6 (NV 3CLpro:22).

■ AUTHOR INFORMATION

Corresponding Authors

*K.-O.C.: phone, 785-532 3849; fax, 785-532 4039; e-mail, kchang@vet.ksu.edu.
*W.C.G.: phone, 316-978 7374; fax, 316-978 3431; e-mail, bill.groutas@wichita.edu.

Notes

The authors declare no competing financial interest.

■ ACKNOWLEDGMENTS

■ ABBREVIATIONS USED

ORF, open reading frame; EDCI, 1-ethyl-3-(3-dimethylaminopropyl)carbodiimide; HOBt, N-hydroxybenzotriazole; DIEA, diisopropylethylamine; DTT, dithiothreitol; DMSO, dimethyl sulfoxide; MNV, murine norovirus; MOI, multiplicity of infection; CPE, cytopathic effect; $TCID_{50}$, the 50% tissue culture infectious dose; IC_{50}, the 50% inhibitory concentration in the enzyme assay; EC_{50}, the 50% effective concentration in cell culture; CC_{50}, 50% cytotoxic concentration in cell-based assays; GESAMT, general efficient structural alignment of macromolecular targets; rmsd, root-mean-square deviation; XDS, X-ray detector software; MME, monomethyl ether

■ REFERENCES

(1) Green, K. Y. Caliciviridae: The Noroviruses. In *Green's Virology*; Knipe, D. M., Howley, P. M., Eds.; Lippincott Williams & Wilkins: Philadelphia, PA, 2007; Vol. *1*, pp 949−979.

(2) Koo, H. L.; Ajami, N.; Atmar, R. L.; DuPont, H. L. Noroviruses: The Leading Cause of Gastroenteritis Worldwide. *Discovery Med.* 2010, *10*, 61−70.

(3) Ahmed, S. M.; Hall, A. J.; Robinson, A. E.; Verhoef, L.; Premkumar, P.; Parashar, U. D.; Koopmans, M.; Lopman, B. A. Global Prevalence of Norovirus in Cases of Gastroenteritis: a Systematic Review and Meta-Analysis. *Lancet Infect. Dis.* 2014, *14*, 725−730.

(4) Hall, A. J.; Lopman, B. A.; Payne, D. C.; Patel, M. M.; Gastanaduy, P. A.; Vinje, J.; Parashar, U. D. Norovirus Disease in the United States. *Emerging Infect. Dis.* 2013, *19*, 1198−1205.

(5) Norovirus. www.cdc.gov/norovirus (accessed January 2015).

(6) Bok, K.; Green, K. Y. Norovirus Gastroenteritis in Immunocompromised Patients. *N. Engl. J. Med.* 2012, *367*, 2126−2132.

(7) Robilotti, E.; Deresinski, S.; Pinsky, B. A. Norovirus. *Clin. Microbiol. Rev.* 2015, *28*, 134−164.

(8) Lee, B. E.; Pang, X.-L. New Strains of Norovirus and the Mystery of Viral Gastroenteritis Epidemics. *CMAJ.* 2013, *185*, 1381−1382.

(9) Hall, A. J. Noroviruses: The Perfect Human Pathogens? *J. Infect. Dis.* 2012, *205*, 1622−1624.

(10) Pringle, K.; Lopman, B.; Vega, E.; Vinje, J.; Parashar, U. D.; Hall, A. J. Noroviruses: Epidemiology, Immunity and Prospects for Prevention. *Future Microbiol.* 2015, *10*, 53−67.

(11) Jones, M. K.; Grau, K. R.; Costantini, V.; Kolawole, A. O.; de Graaf, M.; Freiden, P.; Graves, C. L.; Koopmans, M.; Wallet, S. M.; Tibbetts, S. A.; Schultz-Cherry, S.; Wobus, C. E.; Vinje, J.; Karst, S. M. Human Norovirus Culture in B Cells. *Nat. Protoc.* 2015, *10*, 1939−1947.

(12) Karst, S. M.; Zhu, S.; Goodfellow, I. G. The Molecular Pathology of Noroviruses. *J. Pathol.* 2015, *235*, 206−216.

(13) Thorne, L. G.; Goodfellow, I. G. Norovirus Gene Expression and Replication. *J. Gen. Virol.* 2014, *95*, 278−291.

(14) Blakeney, S. J.; Cahill, A.; Reilly, P. A. Processing of Norwalk Virus Nonstructural Proteins by a 3C-like Cysteine Proteinase. *Virology* 2003, *308*, 216−224.

(15) Hussey, R. J.; Coates, L.; Gill, R. S.; Erskine, P. T.; Coker, S.-F.; Mitchell, E.; Cooper, J. B.; Wood, S.; Broadbridge, R.; Clarke, I. N.; Lambden, P. R.; Shoolingin-Jordan, P. M. A Structural Study of Norovirus 3C Protease Specificity: Binding of a Designed Active Site-Directed Peptide Inhibitor. *Biochemistry* 2011, *50*, 240−249.

(16) Herod, M. R.; Prince, C. A.; Skilton, R. J.; Ward, V. K.; Cooper, J. B.; Clarke, I. N. Structure-based Design and Functional Studies of Novel Noroviral 3C Protease Chimaeras Offer Insights into Substrate Specificity. *Biochem. J.* 2014, *464*, 461−472.

(17) Nomenclature used is that ofthe following: Schechter, I.; Berger, A. *Biochem. Biophys. Res. Commun.* 1967, *27*, 157−162 where S_1, S_2, S_3, ...S_n and S_1', S_2', S_3', ...S_n' correspond to the enzyme subsites on the N-terminus and C-terminus side, respectively, of the scissile bond. Each subsite accommodates a corresponding amino acid residue side chain designated P_1, P_2, P_3, ...P_n and P_1', P_2', P_3', ...P_n' of a substrate or inhibitor. S_1 is the primary substrate specificity subsite and P_1-P_1' is the scissile bond..

(18) Muhaxhiri, Z.; Deng, L.; Shanker, S.; Sankaran, B.; Estes, M. K.; Palzkill, T.; Song, Y.; Venkataraman Prasad, B. V. Structural Basis of Substrate Specificity and Protease Inhibition in Norwalk Virus. *J. Virol.* 2013, *87*, 4281−4292.

(19) Hardy, M. E.; Crone, T. J.; Brower, J. E.; Ettayebi, K. Substrate Specificity of the Norwalk Virus 3C-Like Proteinase. *Virus Res.* 2002, *89*, 29−39.

(20) Someya, Y.; Takeda, N.; Miyamura, T. Characterization of the Norovirus 3C-like Protease. *Virus Res.* 2005, *110*, 91−97.

(21) Mullard, A. 2013 FDA Drug Approvals. *Nat. Rev. Drug Discovery* 2014, *13*, 85−89.

(22) Drag, M.; Salvesen, G. S. Emerging Principles in Protease-Based Drug Discovery. *Nat. Rev. Drug Discovery* 2010, *9*, 690−701.

(23) Tiew, K.-C.; He, G.; Aravapalli, S.; Mandadapu, S. R.; Gunnam, M. R.; Alliston, K. R.; Lushington, G. H.; Kim, Y.; Chang, K.-O.; Groutas, W. C. Design, Synthesis, and Evaluation of Inhibitors of Norwalk Virus 3C Protease. *Bioorg. Med. Chem. Lett.* 2011, *21*, 5315−5319.

(24) Mandadapu, S. R.; Weerawarna, P. M.; Gunnam, M. R.; Alliston, K. R.; Lushington, G. H.; Kim, Y.; Chang, K.-O.; Groutas, W. C. Potent Inhibition of Norovirus 3CL Protease by Peptidyl α-Ketoamides and α-Ketoheterocycles. *Bioorg. Med. Chem. Lett.* 2012, *22*, 4820−4826.

(25) Mandadapu, S. R.; Gunnam, M. R.; Galasiti Kankanamalage, A. C.; Uy, R. A. Z.; Alliston, K. R.; Lushington, G. H.; Kim, Y.; Chang, K.-O.; Groutas, W. C. Potent Inhibition of Norovirus by Dipeptidyl α-Hydroxyphosphonate Transition State Mimics. *Bioorg. Med. Chem. Lett.* 2013, *23*, 5941−5944.

(26) Kim, Y.; Lovell, S.; Tiew, K.-C.; Mandadapu, S. R.; Alliston, K. R.; Battaile, K. P.; Groutas, W. C.; Chang, K. O. Broad-Spectrum Antivirals Against 3C or 3C-Like Proteases of Picornaviruses, Noroviruses, and Coronaviruses. *J. Virol.* 2012, *86*, 11754−11762.

(27) Mandadapu, S. R.; Weerawarna, P. M.; Prior, A. M.; Uy, R. A. Z.; Aravapalli, S.; Alliston, K. R.; Lushington, G. H.; Kim, Y.; Hua, D. H.; Chang, K.-O.; Groutas, W. C. Macrocyclic Inhibitors of 3C and 3C-like Proteases of Picornavirus, Norovirus and Coronavirus. *Bioorg. Med. Chem. Lett.* 2013, *23*, 3709−3712.

(28) Galasiti Kankanamalage, A. C.; Kim, Y.; Weerawarna, P. M.; Uy, R. A. Z.; Damalanka, V. C.; Mandadapu, S. R.; Alliston, K. R.; Mehzabeen, N.; Battaile, K. P.; Lovell, S.; Chang, K.-O.; Groutas, W. C. Structure-Guided Design and Optimization of Dipeptidyl Inhibitors of Norovirus 3CL Protease. Structure-Activity Relationships and Biochemical, X-Ray crystallographic, Cell-based and In Vivo Studies. *J. Med. Chem.* 2015, *58*, 3144−3155.

(29) Lin, J. H. Pharmacokinetics of Biotech Drugs: Peptides, Proteins, and Monoclonal Antibodies. *Curr. Drug Metab.* 2009, *10*, 661−691.

(30) Craik, D. J.; Fairlie, D. P.; Liras, S.; Price, D. The Future of Peptide-Based Drugs. *Chem. Biol. Drug Des.* 2013, *81*, 136−147.

(31) Mallinson, J.; Collins, I. Macrocycles in New Drug Discovery. *Future Med. Chem.* **2012**, *4*, 1409−1438.

(32) Marsault, E.; Peterson, M. L. Macrocyles are Great Cycles: Applications, Opportunities, and Challenges of Synthetic Macrocycles in Drug Discovery. *J. Med. Chem.* **2011**, *54*, 1961−2004.

(33) Giordanetto, F.; Kihlberg, J. Macrocyclic Drugs and Clinical Candidates: What Can Medicinal Chemists Learn from Their properties? *J. Med. Chem.* **2014**, *57*, 278−295.

(34) Mathiowetz, A. M.; Leung, S. S. F.; Jacobson, M. P. Optimizing the Permeability and Oral Bioavailability of Macrocyles. In *Macrocycles in Drug Discovery*; Levin, J., Ed.;Royal Society of Chemistry: Cambridge, U.K., 2015; pp 367−397.

(35) Alex, A.; Millan, D. S.; Perez, M.; Wakenhut, F.; Whitlock, G. A. Intramolecular Hydrogen Bonding to Improve Membrane Permeability and Absorption in Beyond the Rule of Five Chemical Space. *MedChemComm* **2011**, *2*, 669−674.

(36) Rezai, T.; Yu, B.; Millhauser, G. L.; Jacobson, M. P.; Lokey, R. S. Testing the Conformational Hypothesis of Passive Membrane Permeability Using Synthetic Cyclic Peptide Diastereomers. *J. Am. Chem. Soc.* **2006**, *128*, 2510−2511.

(37) Tyndall, J. D. A.; Fairlie, D. P. Macrocycles Mimic The Extended Peptide Conformation Recognized By Aspartic, Serine, Cysteine and Metallo Proteases. *Curr. Med. Chem.* **2001**, *8*, 893−907.

(38) (a) Tyndall, J. D.; Nall, T.; Fairlie, D. P. Proteases Universally Recognize β-Strands in Their Active Sites. *Chem. Rev.* **2005**, *105*, 973−999. (b) Madala, P. K.; Tyndall, J. D.; Nall, T.; Fairlie, D. P. Update 1 of Proteases Universally Recognize β-Strands in Their Active Sites. *Chem. Rev.* **2010**, *110*, PR1−PR31.

(39) Stabile, P.; Lamonica, A.; Ribecai, A.; Castoldi, D.; Guercio, G.; Curcuruto, O. Mild and Convenient One-pot Synthesis of 1,3,4-Oxadiazoles. *Tetrahedron Lett.* **2010**, *51*, 4801−4805.

(40) Xue, C.-B.; He, X.; Roderick, J.; DeGrado, W. F.; Cherney, R. J.; Hardman, K. D.; Nelson, D. J.; Copeland, R. A.; Jaffee, B. D.; Decicco, C. P. Design and Synthesis of Cyclic Inhibitors of Matrix Metalloproteinases and TNF-α Production. *J. Med. Chem.* **1998**, *41*, 1745−1748.

(41) Chang, K.-O.; Takahashi, T.; Prakash, O.; Kim, Y. Characterization and Inhibition of Norovirus Proteases of Genogroups I and II Using a Fluorescence Resonance Energy Transfer Assay. *Virology* **2012**, *423*, 125−133.

(42) Takahashi, D.; Hiromasa, Y.; Kim, Y.; Anbanandam, A.; Yao, X.; Chang, K.; Prakash, O. Structural and Dynamics Characterization of Norovirus Protease. *Protein Sci.* **2013**, *22*, 347−357.

(43) Krissinel, E. Enhanced Fold Recognition Using Efficient Short Fragment Clustering. *J. Mol. Biochem.* **2012**, *1*, 76−85.

(44) Kabsch, W. Automatic Indexing of Rotation Diffraction Patterns. *J. Appl. Crystallogr.* **1988**, *21*, 67−72.

(45) Kabsch, W. *Acta Crystallogr., Sect. D: Biol. Crystallogr.* **2010**, *66*, 125−132.

(46) Evans, P. R. An Introduction to Data Reduction: Space-group Determination, Scaling and Intensity Statistics. *Acta Crystallogr., Sect. D: Biol. Crystallogr.* **2011**, *67*, 282−292.

(47) McCoy, A. J.; Grosse-Kunstleve, R. W.; Adams, P. D.; Winn, M.; Storoni, L. C.; Read, R. J. Phaser Crystallographic Software. *J. Appl. Crystallogr.* **2007**, *40*, 658−674.

(48) Adams, P. D.; Afonine, P. V.; Bunkoczi, G.; Chen, V. B.; Davis, I. W.; Echols, N.; Headd, J. J.; Hung, L.-W.; Kapral, G. J.; Grosse-Kunstleve, R. W.; McCoy, A. J.; Moriarty, N. W.; Oeffner, R.; Read, R. J.; Richardson, D. C.; Richardson, J. S.; Terwilliger, T. C.; Zwart, P. H. PHENIX: a Comprehensive Python-based System for Macromolecular Structure Solution. *Acta Crystallogr., Sect. D: Biol. Crystallogr.* **2010**, *66*, 213−221.

(49) Emsley, P.; Lohkamp, B.; Scott, W. G.; Cowtan, K. Features and Development of Coot. *Acta Crystallogr., Sect. D: Biol. Crystallogr.* **2010**, *66*, 486−501.

(50) Chen, V. B.; Arendall, W. B.; Headd, J. J.; Keedy, D. A.; Immormino, R. M.; Kapral, G. J.; Murray, L. W.; Richardson, J. S.; Richardson, D. C. MolProbity: All-atom Structure Validation for Macromolecular Crystallography. *Acta Crystallogr., Sect. D: Biol. Crystallogr.* **2010**, *66*, 12−21.

(51) Potterton, L.; McNicholas, S.; Krissinel, E.; Gruber, J.; Cowtan, K.; Emsley, P.; Murshudov, G. N.; Cohen, S.; Perrakis, A.; Noble, M. Developments in the CCP4 Molecular Graphics Project. *Acta Crystallogr., Sect. D: Biol. Crystallogr.* **2004**, *60*, 2288−2294.

(52) Evans, P. Scaling and Assessment of Data Quality. *Acta Crystallogr., Sect. D: Biol. Crystallogr.* **2006**, *62*, 72−82.

(53) Diederichs, K.; Karplus, P. A. Improved R-factors for Diffraction Data Analysis in Macromolecular Crystallography. *Nat. Struct. Biol.* **1997**, *4*, 269−275.

(54) Weiss, M. S. Global Indicators of X-ray Data Quality. *J. Appl. Crystallogr.* **2001**, *34*, 130−135.

(55) Karplus, P. A.; Diederichs, K. Linking Crystallographic Model and Data Quality. *Science* **2012**, *336*, 1030−1033.

(56) Evans, P. Biochemistry. Resolving Some Old Problems in Protein Crystallography. *Science* **2012**, *336*, 986−987.